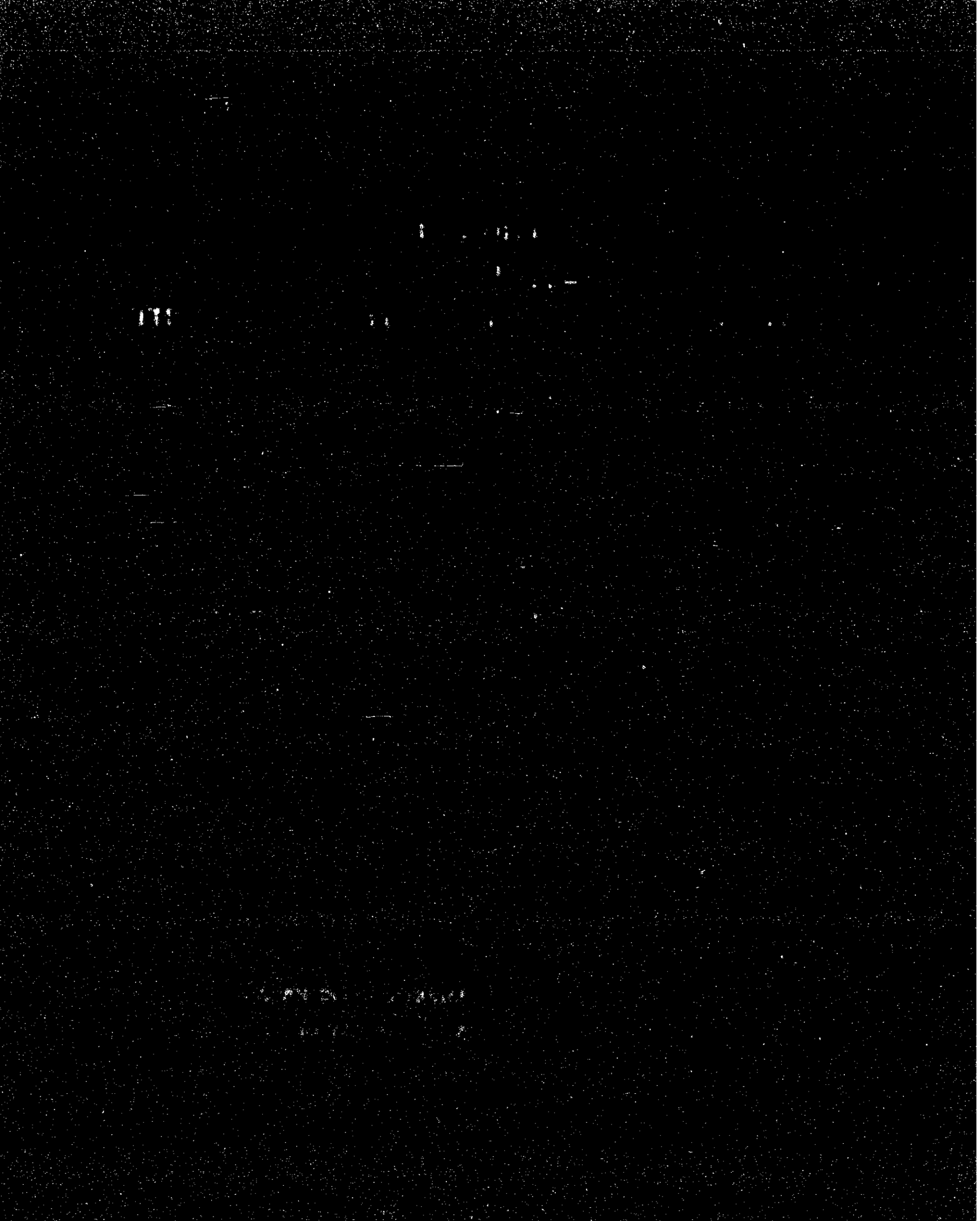

REPORT
ON
THE COOPERATIVE MINERAL EXPLORATION
IN
THE PALMEIROPOLIS AREA
FEDERATIVE REPUBLIC OF BRAZIL

(PHASE Ⅱ)

MARCH, 1988

JAPAN INTERNATIONAL COOPERATION AGENCY

METAL MINING AGENCY OF JAPAN

PREFACE

In response to the request of the Government of the Federative Republic of Brazil, the Japanese Government decided to conduct a mineral exploration in the Palmeirópolis Project and entrusted the survey to the Japan International Cooperation Agency (J.I.C.A.) and the Metal Mining Agency of Japan (M.M.A.J.).

The JICA and MMAJ sent to the Federative Republic of Brazil a survey team headed by Mr. Ikuhiro Hayashi from 18 August to 20 December, 1987.

The team exchanged views with the officials concerned of the Government of the Federative Republic of Brazil and conducted a field survey in the Palmeirópolis area. After the team returned to Japan, further studies were made and the present report has been prepared.

We hope that this report will serve for the development of the Project and contribute to the promotion of friendly relations between our two countries.

We wish to express our deep appreciation to the officials concerned of the Government of the Federative Republic of Brazil for their close cooperation extended to the team.

February 1988

Kensuke Yanagiya

Kensuke Yanagiya
President
Japan International Cooperation Agency

Junichiro Sato

Junichiro Sato
President
Metal Mining Agency of Japan

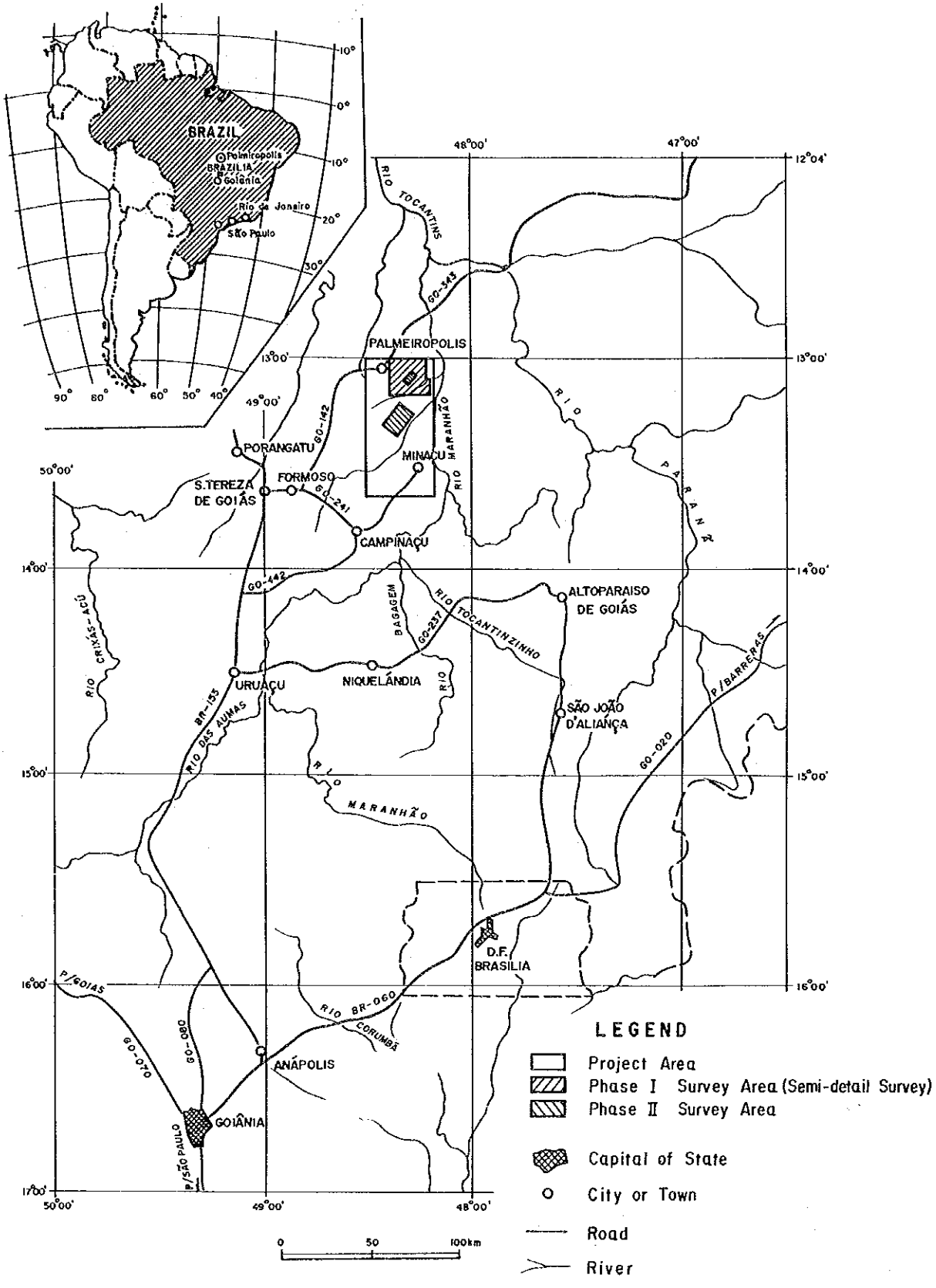

Fig. 1 Location Map of the Project Area

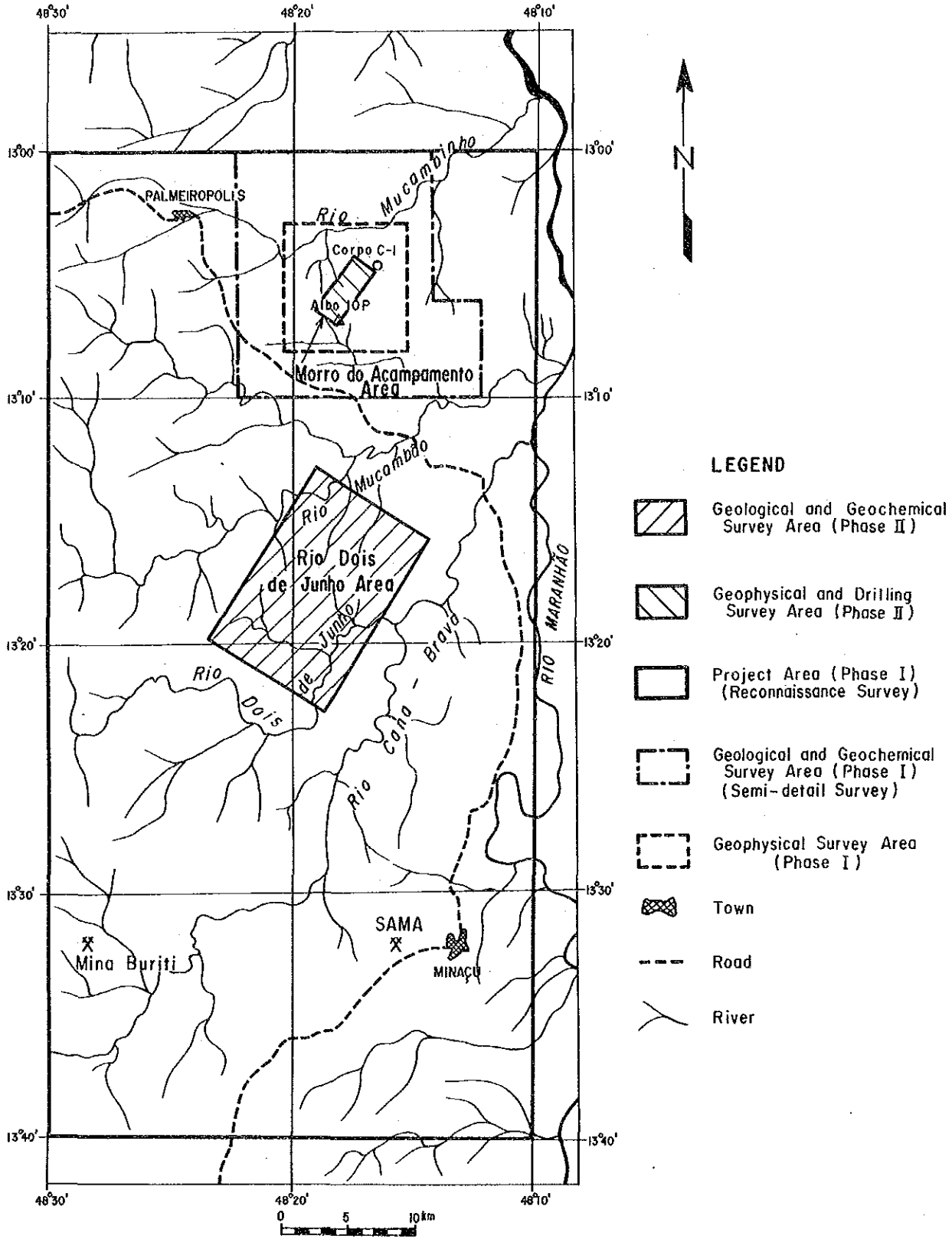

Fig. 2 Location Map of the Surveyed Area

CONTENTS

PART II PARTICULARS

PART III CONCLUSION AND RECOMMENDATION

ABSTRACT

The cooperative mineral exploration in the Palmeirópolis area, the Federative Republic of Brazil, has been conducted for three years starting from 1986 as first phase.

In Phase I, geological survey and geochemical survey for stream sediments were carried out in the whole project area, and geological survey, geochemical survey for soil and geophysical survey with CSAMT and SIP methods were conducted in the area covering the known ore deposits within the project area. Based on the results of the surveys, the Rio Dois de Junho and Morro do Acampamento areas were selected for the follow-up works.

In this Phase II, geological and geochemical soil surveys were carried out in the Rio Dois de Junho area, and geophysical SIP survey and diamond drillings, in the Morro do Acampamento area.

As a results, a geochemical anomalous zone of Cu-Pb-Zn was extracted in the southern portion of the Rio Dois de Junho area by the geochemical survey. But it is too small and suggests a low potentiality for mineral resources.

On the other hand, in the Morro do Acampamento area, IP anomalies were detected at depth to the south of a line 150S in the Block North and a notable IP anomalies which are as good as ones of C-1 ore deposit and trend in N-S direction, were also detected in a low to medium resistivity zone in the Block South.

Three holes, one hole in the north and two in the south, with a total length of 900 meters were drilled. The first hole (MBP-1) near the point of (150S, 85W) with IP anomaly within a high to medium resistivity zone in the Block North could not catch any remarkable mineralization. And the other two drill holes (MBP-2 and MBP-3) in the Block South intersected sulphide mineralization with a maximum of 7 weight percent and thin layers of graphite-quartz schist in amphibolites. However, useful minerals such as chalcopyrite, sphalerite and galena were poorly observed.

Based on the results of the surveys undertaken during the past two phases, additional drillings in the Block South of the Morro do Acampamento area and geophysical SIP survey and drillings in Alvo 10P area were recommended for follow-up works in Phase III.

PART I GENERAL REMARKS

CHAPTER 1 Introduction

1–1 Background of the Survey

By the exploration activities since 1975, it has been clarified that, in and around the Palmeirópolis area, formations of Archaean and Proterozoic age, and acidic and basic to ultrabasic intrusive rocks intruding them are widely distributed, and Cu-Pb-Zn ore deposits such as C-1, C-2 and C-3 exist in the Palmeirópolis volcano-sedimentary sequence which corresponds to a part of the Proterozoic formation.

The cooperative mineral exploration has been conducted for three years since 1986, in the Palmeirópolis area which was selected as a promising area with good potential for mineralization, based on the result of considerating published reports.

During the Phase I, geological survey and geochemical survey using stream sediment were carried out in the whole project area of 2,750 km^2, and geological, soil geochemical surveys and geophysical surveys using CSAMT and SIP methods were in a semi-detailed survey area of 300 km^2, including known ore deposits, within the project area.

1–2 Conclusion and Recommendation of Phase I Survey

1–2–1 Conclusion of Phase I Survey

The conclusions of the Phase I are summarized as follows;

(1) the Palmeirópolis volcano-sedimentary sequence widely distributed in the area is divided into five formations; namely Pip_1 formation of amphibolite, Pip_2 formation of pyroclastic rocks and schistose rocks, Pip_3 formation of amphibolite, Pip_4 formation of intermediate to acidic schistose rocks and Pip_5 formation of pelitic schistose rocks.

(2) the Palmeirópolis deposit (C-1 ore deposit) is formed by the stratiform-lenticular Cu-Pb-Zn ore bodies, harmoniously emplaced between amphibolite (Pip_3 formation) and intermediate to acidic schistose rocks (Pip_4 formation), which are composed mainly of sphalerite, pyrrhotite, pyrite, chalcopyrite and galena.

(3) Geochemical stream sediment analysis in the project area led to extract six anomalous areas as follows;

The semi-detailed survey area and its east.

The area underlain by the Pip_4 vs formation in the central part of the survey area.

The area underlain by the Pip_1 and Pip_3 formations in the central-northeastern part of the survey area.

The area underlain by the Pip_5 formation in the central-northwestern part of the survey area.

The area underlain by the Pm_1 xt and Pmsm formations in the western part of the survey area.

The area underlain by the Pip_3 and Pip_5 formations in the southern part of the survey area.

(4) Based on the results of the soil geochemical survey in the semi-detailed survey area, Pb-Zn anomalous zones arranged in a direction of NE-SW, in the schistose rocks (Pip_4 formation) in Alvo 7P, southeast of 9P and 10P, and Cu-Zn anomalous zones in the eastern part of Alvo 11P, were delineated in addition to a Cu-Pb-Zn high anomalous zone in the vicinity of the C-1 ore deposit.

(5) The geophysical CSAMT method in the semi-detailed survey area indicates that a resistivity structure in the vicinity of the C-1 ore deposit shows a gentle gradient and the similar structures are concentrated around the NE-SW tectonic line through Alvo 7P and 10P.

(6) The result of the SIP method shows that spectral pattern of IP anomaly detected at the western end of the line 150S is similar to that detected around C-1 deposit.

1–2–2 *Recommendation of Phase I Survey*

Based on the results of the Phase I surveys, the following follow-up works have been recommended:

(1) geophysical survey (IP and SIP methods) and drillings in an area from Alvo 7P to the southeast of Alvo 9P

(2) and soil geochemical and geological surveys in the lower valley of Rio Dois de Junho in the central part of the project area.

1–3 Outline of Phase II Survey

The Phase II surveys were carried out in the promising areas where those were extracted based on the results of the Phase I survey.

1–3–1 Survey Area

The survey area is divided into two areas, Rio Dois de Junho and Morro do Acampamento areas.

1–3–2 Purpose of the Survey

The survey was conducted for the purpose of clarifying the geological setting and extracting the promising areas.

(1) Rio Dois de Junho Area

The geological and geochemical soil surveys were done in the Rio Dois de Junho area where Cu-Pb-Zn geochemical anomalies have been obtained by the Phase I stream sediment survey and Pip_4 formation corresponding to the ore bearing horizon is distributed.

The purposes of the surveys were to clarify the distribution of the Pip_4 formation and do the best to find any mineralized showings by the geological survey, and to delineate the anomalies in detail by the geochemical soil survey.

(2) Morro do Acampamento Area

The geophysical SIP survey and diamond drillings were conducted during the Phase II survey period in the Morro do Acampamento area, where Cu-Pb-Zn anomalies have been delineated by the Phase I geochemical soil survey, and resistivity structure and spectral characteristics similar to those in an area involving the known C–1 ore body have been detected at the northeastern corner by the Phase I geophysical SIP and CSAMT surveys.

The purpose of the geophysical survey was to detect similar spectral characteristics in the area similar to that of the know C–1 ore body and the purpose of the drillings was to clarify the source of the spectral characteristics which was thought to be due to probable ore deposit.

1–3–3 Survey Methods

The geological and geochemical surveys were done in the Rio Dois de Junho area, and the geochemical and drilling surveys in the Morro do Acampamento area. Table I–1 shows the substance and quantities of the surveys, and Table I–2 shows the items and quantities of laboratory works.

(1) Rio Dois de Junho Area

The area (150 km^2) is divided into six blocks and the survey within each block was carried out by one geologist of the survey team in cooperation with his Brazilian couterparts.

Geological mapping was carried out concurrently with the geochemical soil sampling, using aerial photos and a drainage map at a scale of 1:10,000 enlarged from a map at a scale of 1:50,000. Because of scarcity of outcrop in the area, the characteristics of soil were fully examined at the time of soil sampling to supplement the geological mapping work.

A total of 2,008 geochemical soil samples were collected not only along the main roads but also along offset survey lines opened by brushing, as in the Phase I survey, to equalize sampling density at 13–14 samples/km^2.

Table I-1 Substance of Survey and Survey Figures

Substance of Survey and Area	Survey Figures	
Geological · Geochemical Survey	Area	150km²
(Semi-detail)	Route Length	560km
	Soil	2,008 samples
Geophysical Survey (SIP Method)	Line Length	16.7km
	Line Numbers	
	11Lines(N : 8.3km, S : 8.4km)	
	Measuring Points	559 points
	Measuring Interval	100m
	Penetration Depth	300m
Drilling Survey	Total Length	900.37m

Table I-2 Items Analysed and Numbers

Items Analyzed and Components	Numbers
Thin Section	30
Polished Section	5
Chemical Analysis	
Ore : Au, Ag, Cu, Pb, Zn, S	10 (60 elements)
Ag, Cu, Pb, Zn, S	10 (50 elements)
Geochemical Analysis	
Soil : Cu, Pb, Zn	2,008 (6,024 elements)
Physical Property	31

(2) Morro do Acampanento Area

The area was divided into two blocks, Block North and Block South, because Morro do Acampamento (Mt. Acampamento) was located at the central part of the area. A geophysical survey using the SIP electrical method, and a drilling survey were conducted in each block.

The SIP electrical survey was conducted by setting survey lines perpendicular to the geological structure. Six survey lines were set on the Block North, and five lines on the Block South. The interval of the survey lines was 200 meters and the interval of the measuring stations was 100 m. The survey lines amount to a total of 16.7 km and measuring stations 559 points. The data collect at each measuring station were processed by a computer installed at the base camp, and the results of computer analysis were further studied on site for the determination of drill site.

Also conducted were the diamond drilling of three holes, one in the Block North (MBP–1, 300 m) and two in the Block South (MBP–2, 3, each hole 300 m), having a total length of 900m.

1–3–4 Organization of the Survey Team

The following table shows the members participated in the planning, consultation and field survey, including geologists and a geophysicist from Departamento Nacional da Produção Mineral (DNPM) and a geologist from Companhia de Pesquisa de Recursos Minerais (CPRM) entrusted by DNPM.

(1) Planning of Survey Project and Consultation

Japanese Team		Brazilian Team	
Kazunori Kano	MMAJ	José Belfort dos Santos Bastos	DNPM
Yozo Baba	MMAJ	Carlos Oiti Berbert	DNPM
Toshihiko Hayashi	MMAJ	Bolivar Gonçalves Siqueira	DNPM
Katsutoki Matsumoto	MMAJ	Walter Hugo Schmaltz	DNPM

(2) Field Survey

Japanese Team

Leader	Ikuhiro Hayashi	Bishimetal Exploration Co., Ltd. (BEC)
Geologist	Norio Ikeda	BEC
Geophysicist	Tsuyoshi Suzuki	BEC
"	Tomio Tanaka	BEC
"	Keiji Tanaka	BEC

Brazilian Team

Leader	Homero Lacerda	DNPM
Geologist	Arpuim Aráujo Pereira	DNPM
"	Valdemar José de Almeida	DNPM
"	José Ribamar Constancio da Silva	DNPM
"	Ivan Wilson Brandão Oliverira	CPRM
Geophysicist	José dos Anjos Barreto	DNPM

1–3–5 Period of Investigation

(1) Geological and geochemical surveys

Period of investigation	August 18, 1987 to October 6, 1987
Period of field survey	August 28, 1987 to September 30, 1987

(2) Geophysical survey

Period of investigation	August 18, 1987 to November 1, 1987
Period of field survey	August 27, 1987 to October 17, 1987

(3) Drilling survey

Period of investigation	October 1, 1987 to December 20, 1987
Period of field survey	October 5, 1987 to December 14, 1987

(4) Report Preparation — October 7, 1987 to February 20, 1988

CHAPTER 2 Geography of the Survey Area

The area is situated to the east to southeast of the Palmeirópolis settlement in Paranã Municipio in the central part of Goiás State. The Palmeirópolis settlement can be reached from Goiania, the state capital city, via Uruaçu and S. Tereza de Goias through State Highway GO-080, National Highway BR-153, and unpaved State Highway GO-142. The total distance between Goiania and Palmeirópolis is 617 kilometers.

The Rio Dois de Junho area being the subject of the geological and geochemical surveys is located 42km south of the Palmeirópolis settlement and it takes about one hour by car.

The Morro do Acampamento area is situated at 20km east of the Palmeirópolis settlement and can be reached in about a half hour's time by car.

2–1 Topography and Drainage

While the area generally shows the topography of gentle hills and flat land, steep cliffs are formed near each river and tributary and on Morro do Acampamento.

Rio Maranhão, the upper stream of Rio Tocantins flows northward through the eastern end of the area, and its tributaries such as Rio Macanbinho, Rio Macambão, Rio Dois de Junho, Rio Cana Brava and Rio Bonito flow eastward crossing through the area.

2–2 Climate and Vegetation

The area is situated at the southern end of the Amazon zone, and belongs to the tropical humid-type climate. The distinction between the rainy season and the dry season is clearly observed. Annual precipitation and temperatures are as follows:

Rainy season	November to March	Precipitation: 1,300 to 1,800mm
Dry season	April to October	Almost no preipitation
Temperature	Annual mean	23° to 24°C
	Maximum	41°C
	Minimum	15°C

The vegetation exhibits the characteristics of cerrado and savanna, with thick growth of shrub and grass. Tall trees as high as more than six meters are also observed in the lateritic low land.

CHAPTER 3 General Geology

The geology of the Palmairópolis area belongs to the Brazil Central shield from the standpoint of global geologic structure of the South American Continent, and consists of metamorphic and volcanic rocks of the Archaean to Proterozoic.

The Proterozoic in which many metalloferous ore deposits of Brazil are found is widely distributed in Goias State.

The main known ore deposits emplaced in the Precambrian formations in Goias State, including the Palmeirópolis area, include Cu-Ni deposits in ultrabasic rock (Niquelandia Deposit and Americano do Brasil Deposit), Asbestos deposit (Cana Brava Deposit), Cu deposit (Mara Rosa Deposit) in basic to acidic volcano-sedimentary metamorphic sequence Cu-Pb-Zn deposit (Palmeirópolis deposit) and Sn-W deposit (Serra da Mesa type) in granitic rocks intruding the above rocks.

The stratigraphy of the Palmeirópolis area is roughly divided into the formations of Archaeozoic and Proterozoic, and the latter is further classified into the lower, middle and upper parts.

The typical stratigraphy of each formation is as follows:

(1) Archaeozoic

Cana Brava basic -ultrabasic rock massif: granulite- basic to ultrabasic complex, granite -gneiss -migmatite complex

(2) Proterozoic

(a) Lower Proterozoic: Palmeirópolis volcano-sedimentary sequence . . . ultrabasic to basic rocks, schist, granite

(b) Middle Proterozoic: Serra da Mesa Group . . . quartzite, schistose rocks, limestone to marble, basic rocks

Rio Maranhão cataclastic zone . . . quartzite, schistose rocks, gneiss

(c) Upper Proterozoic: Paranoa Group . . . quartzite, dolomite, slate, conglomerate

It has been made clear as the result of exploration by DNPM and CPRM (1983, 1984) that the Cu-Pb-Zn deposit in the Palmeirópolis area is emplaced in the Palmerópolis volcano-sedimentary sequence of the lower Proterozoic.

The Palmeirópolis volcano-sedimentary sequence has been further subdivided by CPRM into three units: Unidade de Oeste (western unit), Unidade de Central (central unit) and Unidade de Leste (eastern unit). The application of this classification is limited to the northern part of the survey area, and the classification by DNPM/CPRM(1983) was more effective for the whole area;

that is, the sequence is divided, from the base upward, into Pip_1, Pip_2, Pip_3, Pip_4 and Pip_5. The palmeirópolis ore deposit is emplaced between Pip_3 and Pip_4 formations.

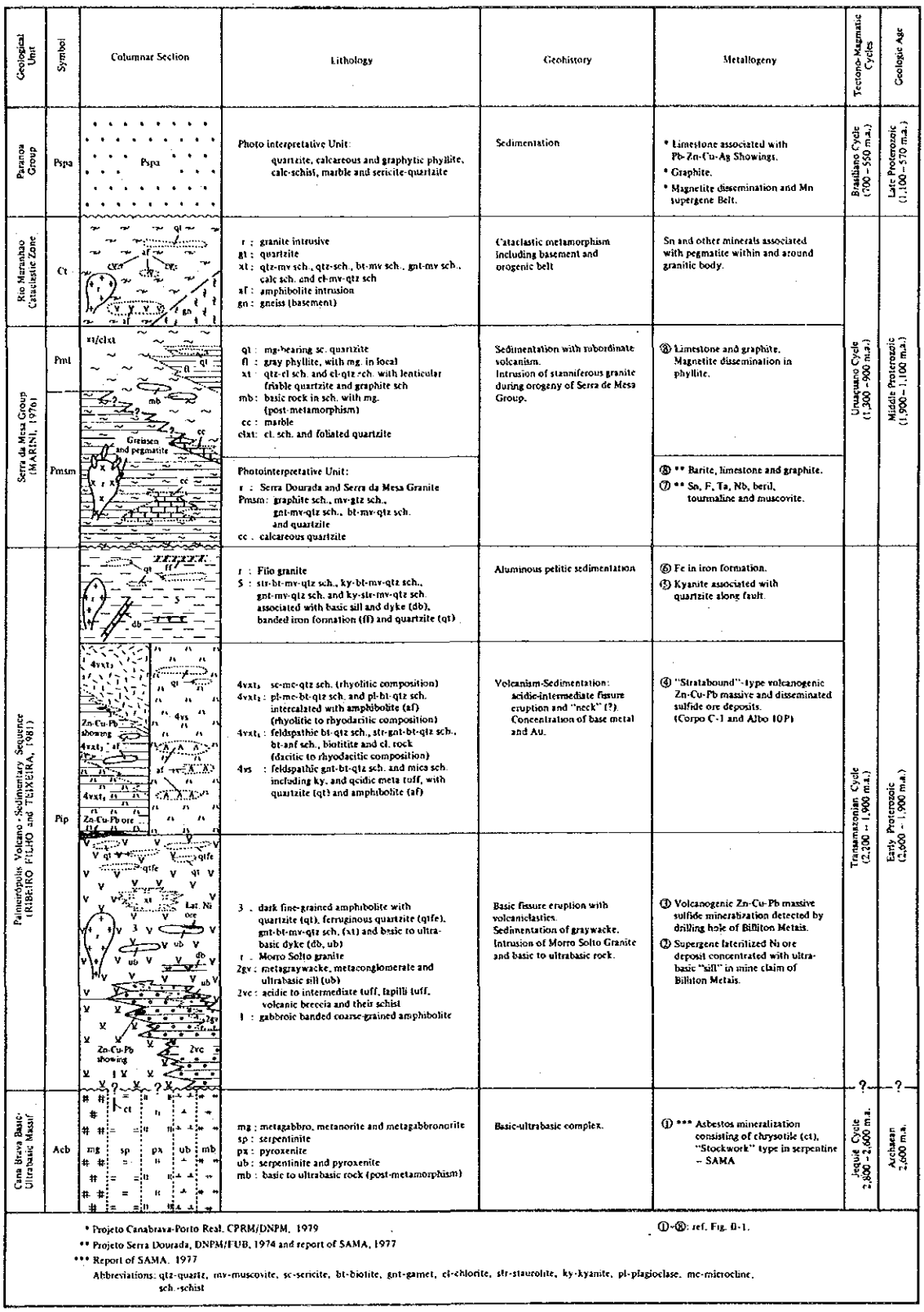

Fig. I-3-1 Generalized Stratigraphic Columnar Section in the Project Area

CHAPTER 4 Overall Discussion on Survey Results

4–1 Rio Dois de Junho Area

The known ore deposit (C-1) is understood to be emplaced in the Pip_4 formation immediately above the Pip_3 formation. The purpose of the surveys were to clarify the distribution of the Pip_4 formation and do the best to find any mineral showing by the geological survey, and to delineate the anomalies related to the mineralization by the geochemical soil survey.

As the results of the surveys, the distribution of schists occupying the most part of the Pip_4 formation, and the distribution of amphibolites which form the Pip_1 and Pip_3 formations and are interbedded into the Pip_4 formation were clarified in detail (see Fig. II–2–1).

The Pip_3 and Pip_4 formations are widely distributed in the central to eastern parts and occupy about two-thirds of the surveyed area. Schists of the Pip_4 formation show two zones with widths of 1 to 1.5 km, amphibolites forming the Pip_1 and Pip_3 formations and a part of Pip_4 formation show three zones with widths of 1.5 to 3 km. The zones are elongated in nearly parallel with each other, trending NE-SW direction in the northeastern part and N-S direction in the southern part.

Only a mineral showing was observed around a boundary between the Pip_3 and Pip_4 formations. There, a lot of gossan floats with a maximum diameter of 1.0m are scattered.

According to the result of the geochemical survey (Fig. II–2–3), the score distributions of the first factor successfully explain the lithological distributions in the area; distributions of high scores of 1.0 or more, extending NE-SW in the northeastern part and N-S in the southern part, coincide with the distributions of amphibolites.

On the other hand, high scores of not less than 1.0 of the second factor supposed to be related to a type of mineralization are not concentrated much and have no remarkable trend, although they are observed more in the southwest than in the northeast.

Two small areas were delineated in an area underlain by the Pip_4 vs formation in the southern part, for the reason that the areas are overlapped by high anomalies for Cu, Pb and Zn and high scores of the second factor.

However, there is few possibility of the same type of mineralization as that of the Palmeirópolis ore deposit, in the Rio Dois de Junho area, because the high score distributions of the second factor might be parallel with the amphibolite distributions, if the second factor is related with the same type of mineralization as the Palmeirópolis ore deposit supposed to be syngenetic and no remarkable mineralization is recognized.

4–2 Morro do Acampamento Area

The results of the geophysical survey and drillings carried out in this Phase II are synthetically discussed together with the geological and geochemical soil surveys results conducted in the past Phase I, of which a brief summary is given, in addition to that of the geophysical survey and drillings results.

4–2–1 Geology, Ore deposit and Geochemical Anomaly

The geology of the area is composed of the Pip_3, Pip_4 and Pip_5 formations in the Palmeirópolis volcano-sedimentary sequence of early Proterozoic age, and shows complicated structure blocked by faults trending NE-SW and NW-SE.

In the Block North, mica-quartz schist of the Pip_4 formation are widely distributed and in the Block South, mica-quartz schist, amphibolites and graphite-quartz schist of the Pip_4 formation and mica-quartz schist of the Pip_5 formation are distributed.

The Pip_4 formation in which the C-1 ore deposite is emplaced immediately above the Pip_3 formation is significant for ore horizon in the area. The Alvo 10P in the southwestern part of the area is also located in an area underlain by the Pip_4 formation. Although the C-2 and C-3 ore deposits located beyond the northern limit of the project area, were before believed to be emplaced in the same horizon as the C-1 ore deposit, it is clarified by current exploration of CPRM that they are overlain by the iron formation correlated with the uppermost of the Pip_4 formation.

The geological background of the Block South, confirmed by the two drill holes, is similar to the geology around the C-2 and C-3 ore deposits.

The geochemical soil survey in the past Phase I shows that the geochemical anomalous areas of Cu-Pb-Zn extracted are aligned with NE-SW direction, from the C-1 ore deposit to the Alvo 10P.

4–2–2 *Results of Geophysical Survey*

Resistivity distribution of this area shows a general trend of N–S ~ NNE–SSW. IP anomalies were detected, one in Block North and two in Block South.

High resistive zones with a resistivity of more than 1000 ohm-m are seen in the western and eastern part of Block North, both of which correspond with quartz rich formations.

The western resistive zone is distributed along Morro do Acampamento in NE–SW direction in the center corresponding with $Pip_4 vxt_2$. While the eastern one extending in the deep zone in NW–SW direction meet with the western resistive zone in Block North corresponding with

$Pip_4\,vxt_1$. This seems to become deeper towards south.

Medium resistivity of 500 ~ 1000 ohm-m corresponds with Pip_3 amphybolite and Pip_4vxt_1 seen in the north, which suggest that Pip_3 and $Pip_4\,vxt_1$ are widely distributed to the north of the survey area.

In so far as Block South, high resistivity are seen in the eastern part of the area while low-medium resistivity are seen in the west. The boundary of those resistivity blocks shows an eminent resistivity contrast, which makes it easy to identify a fault structure or a boundary. The biggest inferred fault is found in the central area running in NE–SW direction. Several small scale faults trending in NW–SE or N–S are also seen, running across the biggest fault at low angles.

Middle resistivity in the west of the Block South correspond with amphibolites, while low resistivity of less than 100 ohm-m to graphite schist respectively, however, the general resistivity change seems to be reflecting the complex geological structure such as folding and faulting structure.

Geological circumstance of this region is so complicated that the variable IP responses make the interpretation difficult.

IP anomalies in Block North are detected in middle to high resistivity zone which correspond with N–S trending $Pip_4\,vxt_1$ and Pip_3. According to the model simulation done in the Phase I Survey, a rich sulphide mineralization was assumed under 250m from the ground surface on Line 150S, showing a tendency of dipping towards south. IP anomalous source detected near Line 150S are considered to be due to lateral effect of sulphide dissemination on Line 160S. It seems that a rich sulphide mineralization is not a massive ore but a disseminated zone.

IP anomalies detected in Block South are seen separately in middle resistivity zone and in high resistivity zone. The former indicates the east dipping patterns, whose spectral patterns are of sulphide mineralization affected by graphite schist. An exploration drilling conducted for this anomaly revealed that the IP anomalous source is not condensed sulphide mineralization but both effect of graphite schist and sulphide minerals.

The latter spectral pattern was considered to be due to sulphide minerals, however, judging from the distribution pattern of IP anomalies and PFE, it is inferred that the anomalies seem to be caused by weak dissemination of sulphide minerals.

4–2–3 Results of Drilling

Based on the results of geophysical and geological surveys, three drilling holes with a total drilling depth of 900.37m were carried out.

No promising ore body was confirmed in this year, but SIP anomalous source and the geological structure were clarified by those drillings.

(1) MBP−1

This hole mainly penetrated mica-quartz schist. It was difficult to decide that chlorite-biotite-amphibole schist seen at the depth of 103.50 ~ 122.00m are either the intercalation of Pip_4 vxt$_1$ formation or amphibolites in Pip_3 formation, but judging from the geology of the area, they are categorized in Pip_4 vxt$_1$ formation as the thickness is thin that quartz and biotite are more abundant in the rock than Pip_3 formation. Mineralogical analysis of the cores indicate that content of sulphide minerals is less than 1%. Physical property test of the cores also show a weak P.F.E. with no IP anomalous source being detected in the cores.

(2) MBP−2, 3

Both holes penetrated mica-quartz-amphibole schist (amphibolites), amphibolites intercalated by graphite-quartz schist and garnet-staurolite-mica-quartz schist.

It is inferred that graphite-quartz schist bearing zone and the schistose rocks below its horizon seem to continue to the shallow zone of graphite-quartz schist and schist of Pip_5 formation, and this results agrees well with the geophysical interpretation.

Based on the above mentioned facts and the surface geology, geological structure of this area, it is interpreted to be in the recumbent folding.

According to assay results of the drilling cores, total sulphide minerals at the richest mineralized zone of pyrite and pyrrhotite is 7 weight percent in maximum, where P.F.E. values are high in this zone. IP anomalies detected in Block South seem to be caused by pyrite, pyrrhotite and graphite.

CHAPTER 5 Conclusion and Recommendation for Phase III Survey

5–1 Conclusion

Rio Dois De Junho Area

A sporadical geochemical anomalous zone of Cu-Pb-Zn was extracted in the southern portion of the area. However it seems difficult to expect ore deposits of the same type of the Palmeiropolis'. Even if existed, it is presumed to be of a small scale.

Morro do Acampamento Area

(1) The hole (MBP-1) was drilled in order to verify the IP anomaly which was detected below around the point 85W of line 150S in the Block North. But no remarkable mineralization was intersected.

(2) Strong IP anomalies with almost the same magnitude as ones of C-1 deposit, and trending N-S, were detected in a low to middle resistivity zone in the Block South.

(3) In order to verify the IP anomalies between points of 270W and 280W of line 270S, and between points of 260W and 270W of line 310S, the drillings of MBP-2 and MBP-3 were conducted. As a result, dissemination of sulphide minerals (mainly composed of pyrite and pyrrhotite) with a maximum weight percent of 7 and thin layers of graphite-quartz schist, were intersected in amphibolites, with widths of 70m and 100m, but useful minerals such as chalcopyrite were found a little.

5–2 Recommendation for Phase III survey

The graphite-quartz-schist intersected by the drillings in the Block South is probably correlated with the iron formation overlying the C-2 and C-3 ore deposits, so that there is still a possibility that the ore horizons of the C-2 and C-3 deposits may exist in the Block South.

As the Alvo 10P area has not provided us enough information from the depth though many informations on geochemical, geophysical (IP), and shallow drilling data have been obtained through CPRM, follow-up surveys to collect information from the depth are expected.

Therefore, in Phase III, the following follow-up surveys are recommended to be carried out in the Morro do Acampamento area.

(1) Drilling for the final evaluation of the Block South.

(2) Geophysical SIP survey and Drilling for collection of informations at depths in the Alvo 10P area.

PART II PARTICULARS

CHAPTER 1 Outline of the Survey

The geological and soil geochemical surveys were carried out in the Rio Dois de Junho area (150 km^2). The geophysical and drilling surveys were conducted in the Morro do Acampamento area.

1–1 Field Procedure

1–1–1 Geological and Geochemical Surveys

Geological mapping at a scale of 1:10,000 was done using a drainage map at 1:10,000 enlarged from the 1:50,000 scale map, and air photographs at 1:25,000.

Concurrently, two thousand and eight soil samples were collected at the average sampling density of 13 to 14 samples per square kilometer (PL. II–1–1). The sampling was carried out along the main roads and rivers. In addition, offset survey lines were set by clearing in order to make distribution of sampling stations as even as possible over the whole area. Sample numbers, colors, constituents of soil, sampling depths and geological units were recorded at each sampling station for the geological mapping work.

The areas sampled were divided into six blocks with respective block numbers, and the block number of each sample was also recorded together with the sample number.

The samples collected were chemically analyzed by the atomic absorption method for the following three target components: Cu, Pb and Zn.

Fig.A–1 shows the location of rock and ore samples and Tables A–1 and A–2 show the results of microscopic observation.

1–1–2 Geophysical Survey

(1) Purpose

In the Morro do Acampamento area, the resistivity structure was clarified and the promising zone for the mineralization were delineated by the CSAMT method, and the spectral pattern of the C-1 ore body was understood by the SIP method in the last phase.

In this phase, the SIP electrical method was adopted in order to locate the drilling points by means of understanding the distribution of the spectral pattern similar as that at the C-1 ore body (caused by the sulfide minerals) in the promising zones delineated from the resistivity structure, in the geological/geochemical anomalous zones and in the SIP anomalous zones.

(2) Method

The SIP method is a similar one as IP. The difference between both methods is the range of frequencies used, that is, the frequency-domain IP method adopts only two frequencies, but

PALMEIRÓPOLIS

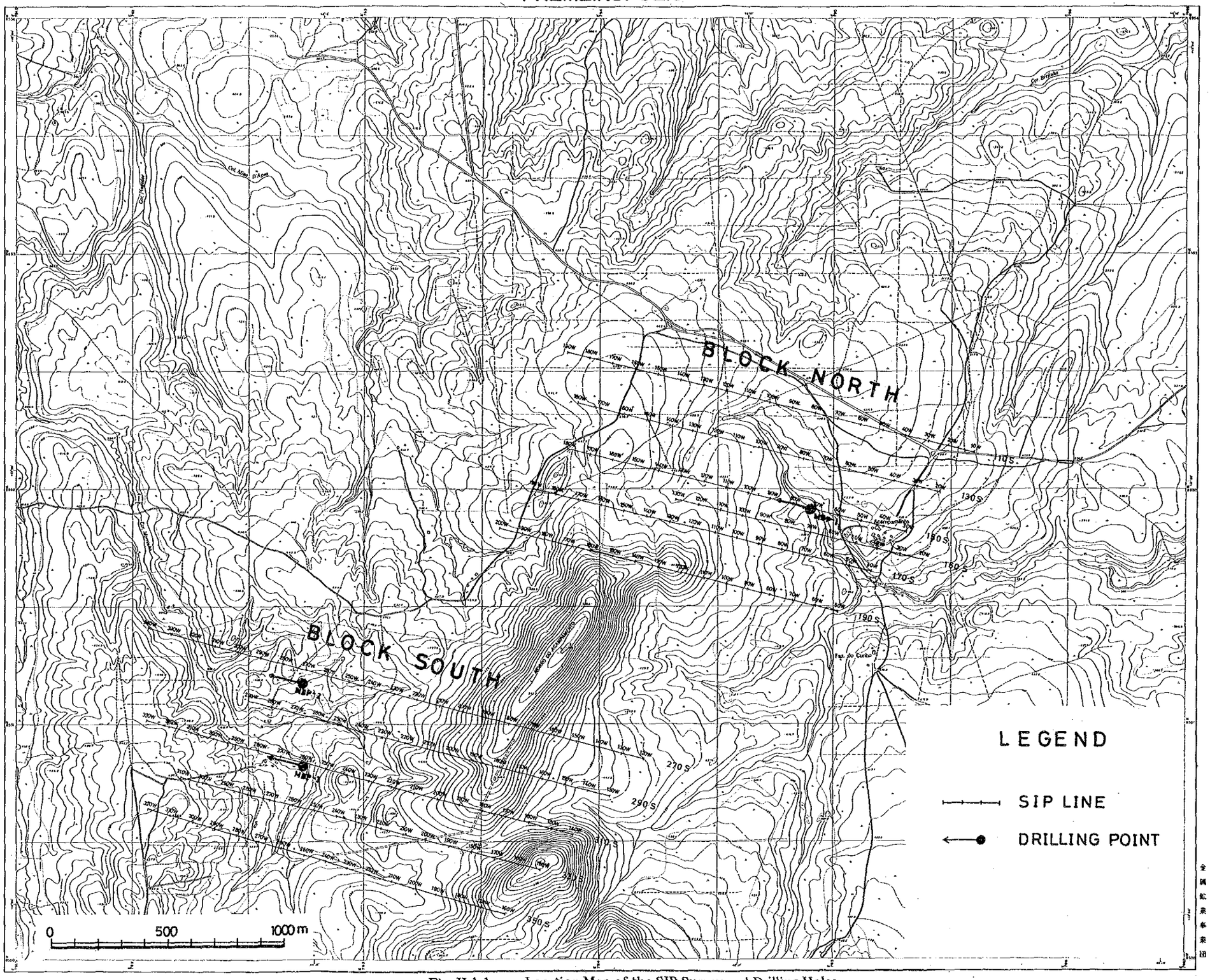

Fig. II-1-1 Location Map of the SIP Survey and Drilling Holes

the SIP method utilizes multi-frequencies between 0.1 Hz and 100 Hz. In this survey, 42 frequencies between 0.125 Hz and 88 Hz were adopted, and magnitudes and phase-differences for each frequency were measured. The electrode configuration employed was a dipole-dipole arrangement and the electrode spacing was 100m.

The area surveyed is consisted of two blocks, which are located at the northern and southern parts of the Morro do Acampamento running in the N-S direction. In the following sections, two blocks are called "Block North" and "Block South", respectively. In both blocks, 11 SIP survey lines in total were settled at 200m apart each by means of the open traverse surveying method as shown in Fig. II−1−1, and communication lines were also set at 25m apart from the main SIP survey lines as shown in Fig. II−1−2.

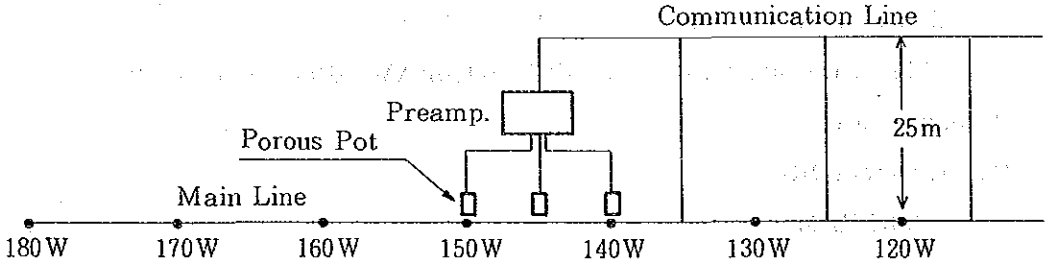

Fig. II-1-2 Electrodic Configuration

Table II−1−1 Specification and Survey Amount of SIP Survey

Area	Line	Length	Points	Electrode Spacing	Electrode Separation Factor
Northern Block	Line 110S	1,500m	46 pts		
	Line 130S	1,500m	48 pts		
	Line 150S	1,500m	49 pts		
	Line 160S	800m	28 pts	a=100m	n=1~5
	Line 170S	1,500m	49 pts		
	Line 190S	1,500m	49 pts		
Subtotal	6 lines	8,300m	269 pts		
Southern Block	Line 270S	2,100m	79 pts		
	Line 290S	1,500m	49 pts		
	Line 310S	1,800m	64 pts	a=100m	n=1~5
	Line 330S	1,500m	49 pts		
	Line 350S	1,500m	49 pts		
Subtotal	5 lines	8,400m	290 pts		
Total	11 lines	16,700m	559 pts		

(3) Survey Instruments

In this survey, the instrument system, made by Zonge Engineering & Research Organization (U.S.A.), was adopted, which is shown below and Fig. II–1–3.

1) Transmitting part

Engine generator (ZMG-10)

Output power 10 KVA/3,200 rpm, 400 Hz, 3-phase

Transmitter (GGT-06)

Output power 10 KVA, 20A, 1,000V

Frequency DC-12 KHz

2) Receiving part

Data Processor (GDP-12)

Frequency 1/16 – 2,048 Hz

Minimum input voltage 0.2V/1,024 stacking

12-bit A/D converter & 16-bit MPU, 16 KBRAM, 50/60 Hz notch filter

3) Recording part

Data recorder (DR-1)

500 KBRAM

1–1–3 Drilling Survey

The drilling survey was conducted in the Morro do Acampamento area. Drilling was performed by GEOSOL (Geologia e Sondagens LTDA.), a local prospecting company, using two drill machines.

Table A–4 shows the generalized drilling results, and Table A–5 shows the machines, consumed materials and their amounts, as well as the use of diamond bits.

(1) Locations of Drill Site (Fig. II–1–1)

Three drill sites were selected, based on the results of the geophysical survey. The first hole (MBP–1) was collared in the Block North. The second (MBP–2) and the third (MBP–3) holes were collared in the Block South.

The following table shows the exact locations of the three drill sites.

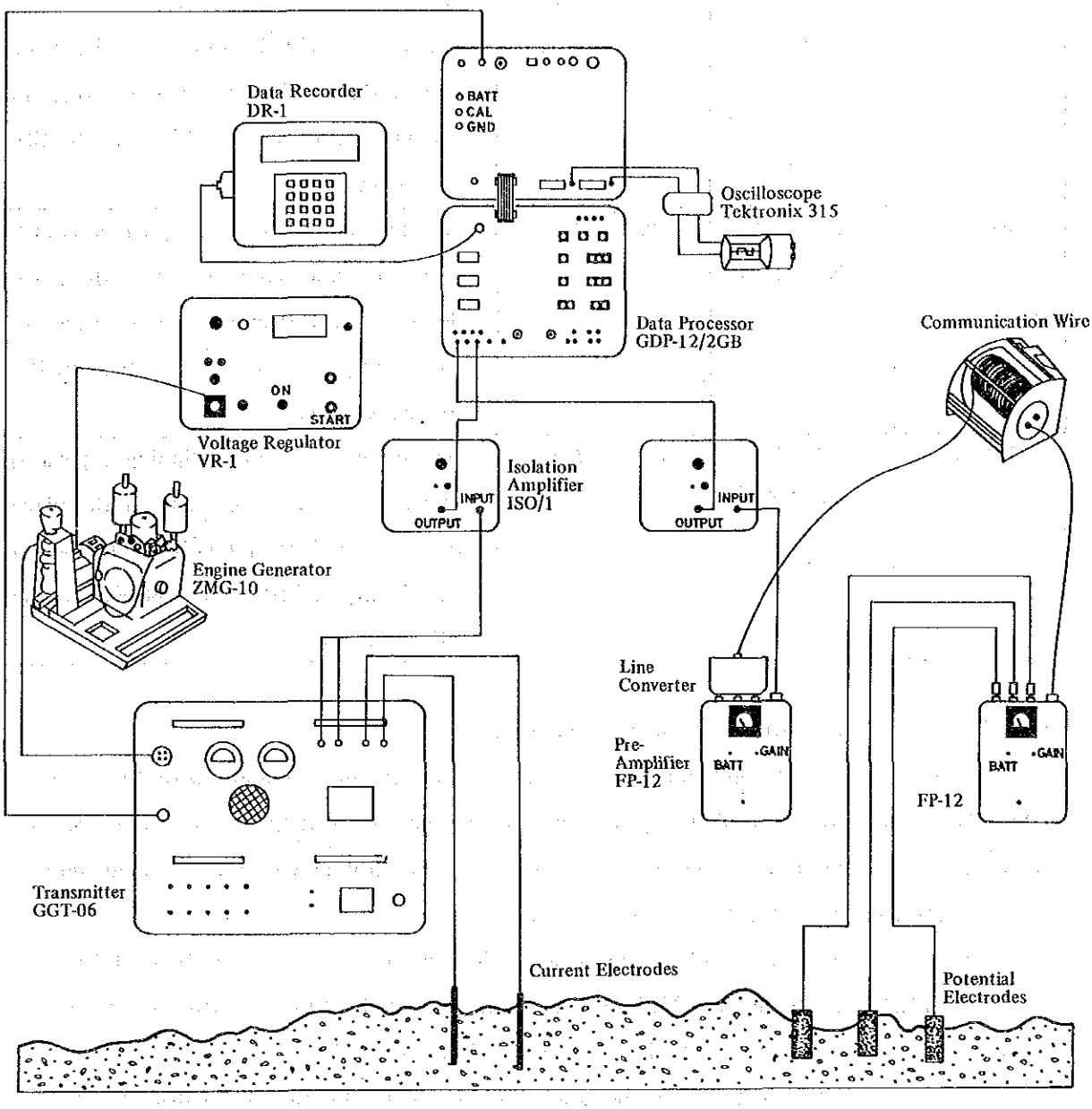

Fig. II-1-3 Diagram of SIP Survey System

Drill Holes	Location	Azimuth and Inclination	Anomalous Sources to Be Confirmed
MBP–1	E794.90 N8551.91	285° –60°	An anomalous source dipping eastward, which is expected to occur at the place deeper than 150 meters below surface in the vicinity of 150S 85W along the SIP survey lines.
MBP–2	E792.73 N8551.17	285° –60°	An anomalous source dipping eastward, which is expected to occur at the place deeper than 150 meters below surface in the vicinity of 270S 270–280W along the SIP survey line.
MBP–3	E792.73 N8550.82	285° –60°	An anomalous source dipping eastward, which is expected to occur at the place deeper than 150 meters below surface in the vicinity of 310S, 270–280W along the SIP survey line.

(2) Transportation of Drilling Equipment and Supplies

It was instructed beforehand that the survey team should negotiate with the staff of GEOSOL in charge of the drill survey to decide on the main lines of the transportation plan of the drilling equipment and supplies into Palmeirópolis so that drilling work might immediately be started as soon as drilling locations were determined.

Although a new access road was constructed this time for a distance of about 200 meters from the CPRM camp to the hole MBP–1, the existing road and the one constructed for the geophysical survey of this time were used to reach MBP–2 and MBP–3.

Therefore, the transportation of the equipment after determination of the drilling locations was carried out by truck in a relatively short period of time.

(3) Leveling of Ground

A bulldozer was used for leveling of the ground at the site of the hole MBP–1 at the time of construction of the access road, but it was not necessary to use dozer for preparation of the sites for the holes MBP–2 and MBP–3.

(4) Water for Diamond Drilling

There was a stream one to two meters wide in the vicinity of each hole; one about 50 meters from the hole MBP–1 and the other two about 400 meters and 100 meters from the holes MBP–2 and 3 respectively. Water was fed from these streams using pumps. Although these streams are dried up during the dry season, sufficient water was available this time because it was the beginning of the rainy season.

The surrounding areas of the drill holes were generally flat and no head higher than 10 meters was found in these places.

(5) Drill Work

The overburden was penetrated at each hole by the conventional method using the NW metal bit. After encountering the bed rock, drilling was performed by the conventional method using the HX or NX diamond bits.

The status of drilling of each hole is as follows (Fig. II–1–4(1~3)).

MBP–1

0 ~ 11.55 m :

The surface soil and highly weathered rock (mica-quartz schist) were cut by the conventional method using the NW metal bit.

11.55 ~ 20.90 m :

Mica-quartz schist was cut by the conventional method using the HX diamond bit, which was replaced with the NX diamond bit at 20. 90 m.

20.90 ~ 300.15 m :

Mica-quartz schist, amphibole schist, and chlorite-mica-quartz schist were drilled by the conventional method using the NX diamond bit. The rock facies were stable and the drilling was performed favorably until the water pump became out of order at 249.70 m. After spending one whole day for repairing at this point, the drilling was completed at the planned depth, followed by the measurement of the dip of the hole. The equipment was then moved to the site of the hole MBP–3 on November 4.

MBP–2

0 ~ 17.10 m :

The surface soil and highly weathered rock was cut by the conventional method using the NW metal bit. The pump was adjusted and replaced at 15.90 m.

17.10 ~ 21.45 m :

Weathered rock (amphibolite) was cut by the conventional method using the HX diamond bit.

21.45 ~ 300.12 m :

Amphibole schist, graphite schist, and mica schist were drilled by the conventional method using the NX diamond bit. Sulfide dissemination zones were encountered in the section between 99.50 m and 168.20 m. The drilling was performed favorably, and the hole was completed after reaching the planned depth.

MBP–3

0 ~ 13.70 m :

Surface soil was penetrated by the conventional methods using the NW metal bit.

13.70 ~ 300.10 m :

Amphibole schist, graphite schist and mica schist were cut by the conventional method using the NX diamond bit. Sulphide dissemination zones were encountered in the section between 56.00 m and 162.50 m. The drilling was performed favorably, and the hole was completed after reaching the planned depth.

(6) Survey of Deviation of Drill Holes

The survey of deviation of drill holes was carried out using Tro-Pari survey instrument in order to grasp accurately the information on deviation. As a result, the dips of the holes were almost as those innitially planned and the maximum angle of deflection was four degrees as shown below. Errors of surveyed values of azimuth however were great due to the effect of pyrrhotite.

Hole MBP–1 (Planned Dip: –60°)

Surveyed depth	Dip	Azimuth
50 m	61°	306°
100 "	62°	314°
150 "	63°	322°
200 "	63°	318°
250 "	61°	280°
300 "	60°	269°

Hole MBP–2 (Planned Dip: –60°)

Surveyed depth	Dip	Azimuth
50 m	61°	288°
100 "	61°	249°
150 "	60°	274°
200 "	59°	287°
250 "	58°	249°
300 "	56°	253°

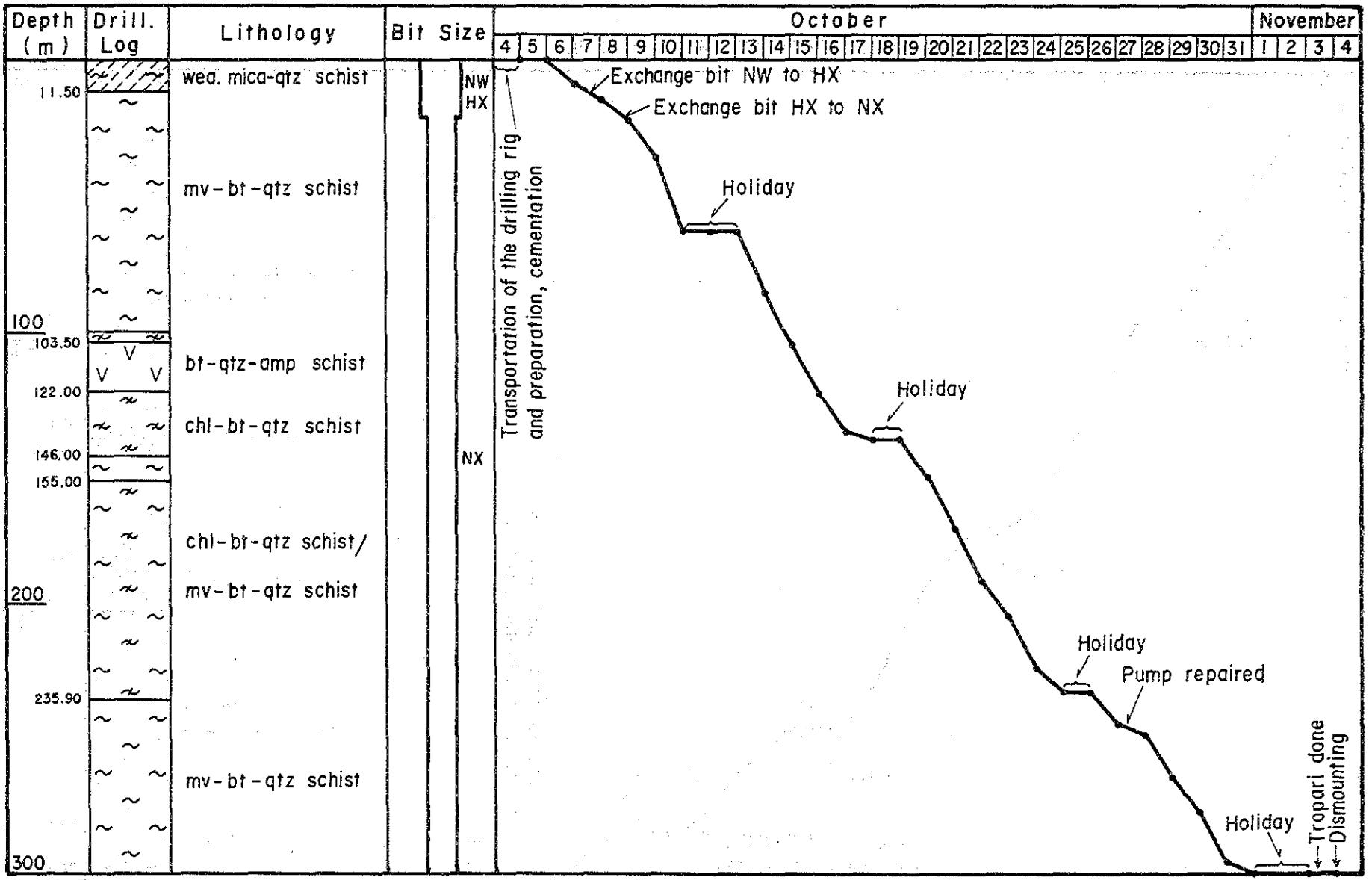

Fig. II-1-4 (1) Progress Record of Hole MBP-1

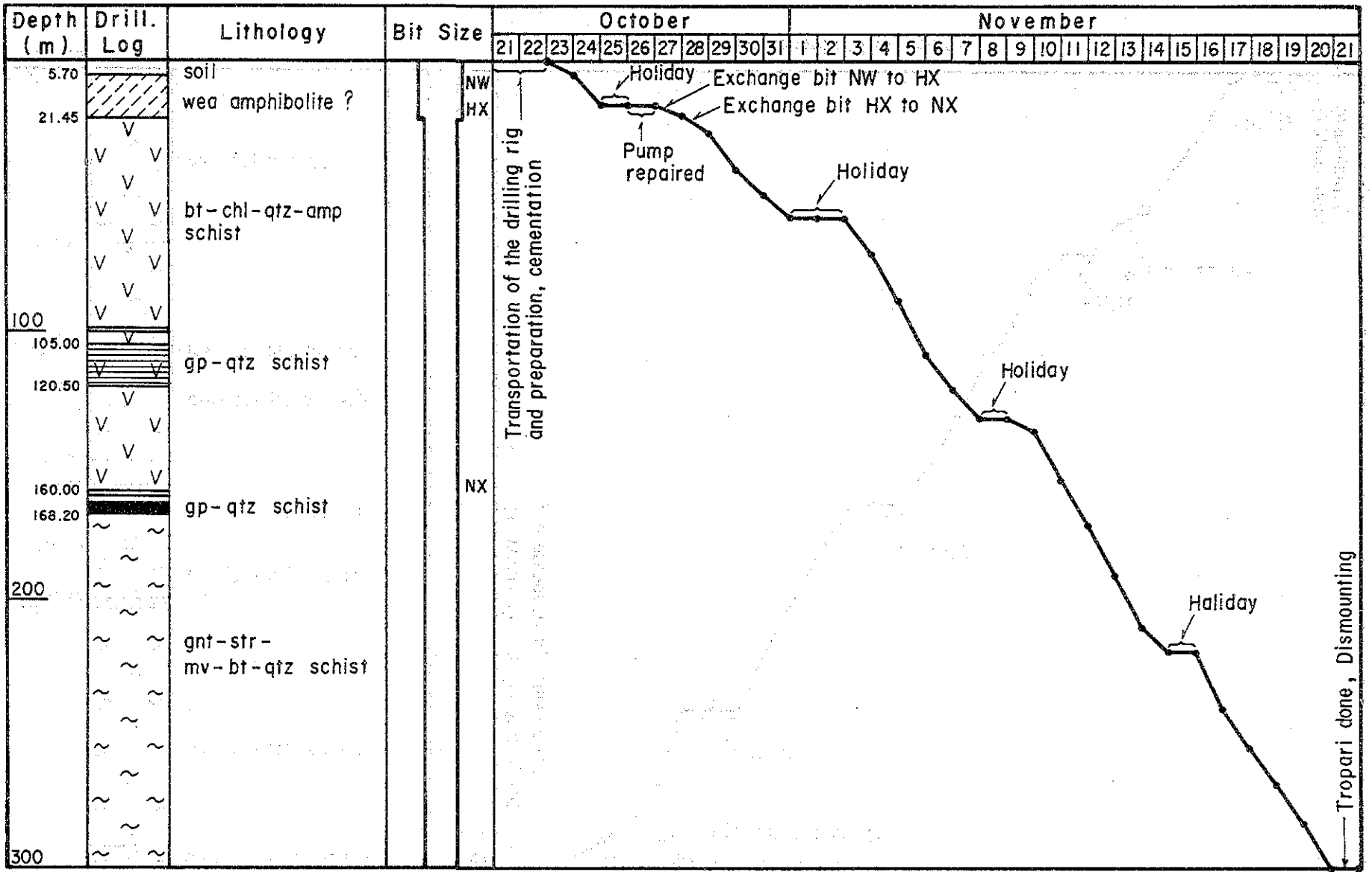

Fig. II-1-4 (2) Progress Record of Hole MBP-2

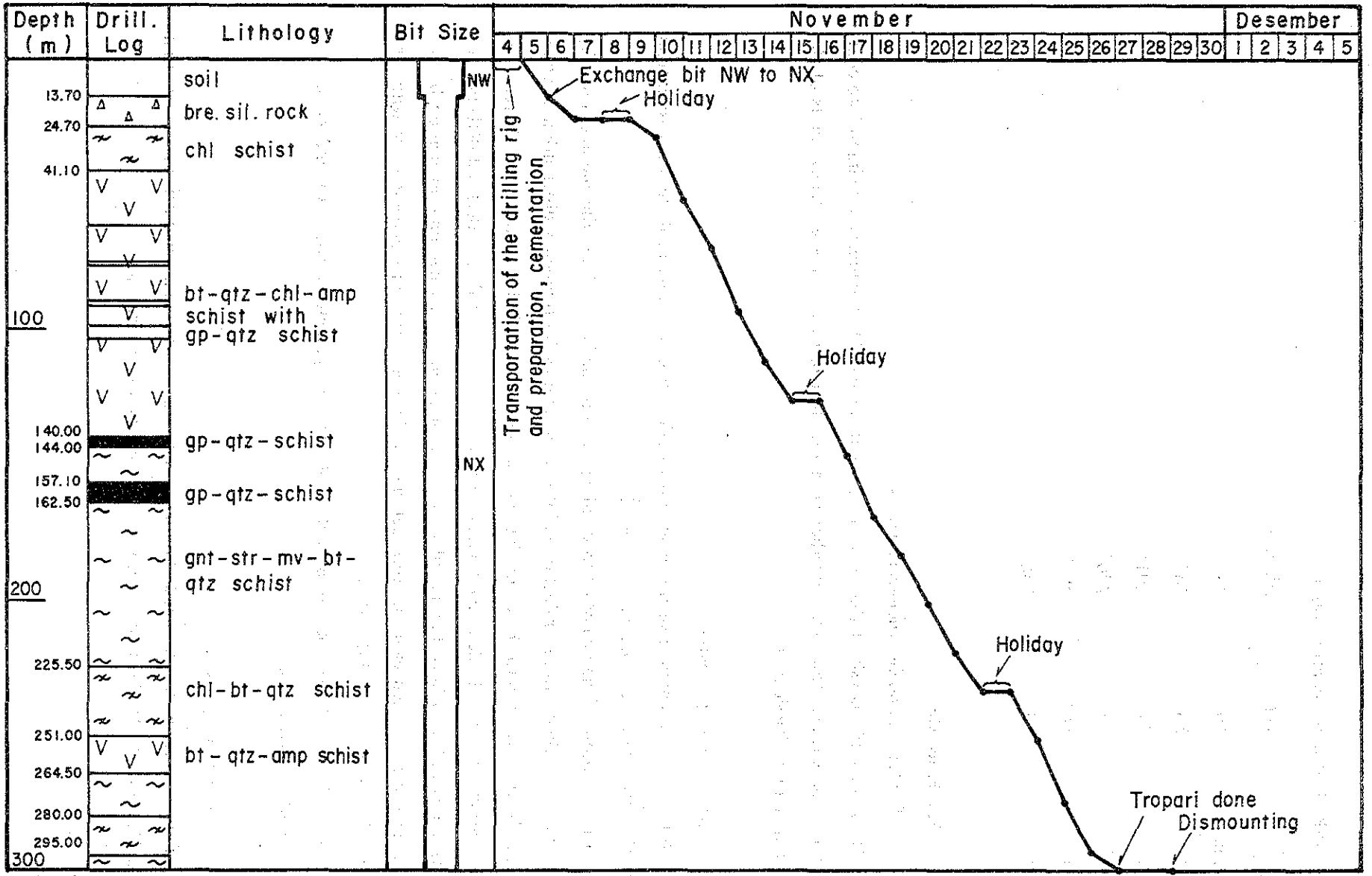

Fig. II-1-4 (3) Progress Record of Hole MBP-3

Hole MBP–3 (Planned depth: –60°)

Surveyed depth	Dip	Azimuth
50 m	59°	287°
100 "	58°	267°
150 "	57°	291°
200 "	57°	290°
250 "	56°	287°
300 "	56°	286°

1–2 Data Processing

1–2–1 Geological and Geochemical Surveys

The results of analysis of the three components of the 2,008 samples were input into computer and statistically processed, together with the data related to the geological units of the sampling stations (Table A–6).

(1) Single Component Analysis

Histograms and cumulative frequency distribution diagrams were made in order to extract anomalous values of each component (Figs. II–1–5).

Determination of anomalous threshold value was made based on the method used by Sinclair (1974). Owing to the inflection point in each cumulative frequency distribution diagram, Cu and Zn are divided into three populations: anomalous population (hereinafter referred to as A polulation) and two background populations (hereinafter referred to as B(I) and B(II) populations). Pb was divided into two populations: A population and background population B. The threshold values of each element were determined by comparing one percent value with 99% value of each population (Table II–1–2).

Table II–1–3 shows correlation matrix of each component, in which Cu and Zn show a strong positive correlation.

(2) Multivariate Analysis

Two factors were extracted by factor analysis in the same manner as in the first phase (Table II–1–4). The first factor is Zn-Cu, and the second Pb-Cu(-Zn).

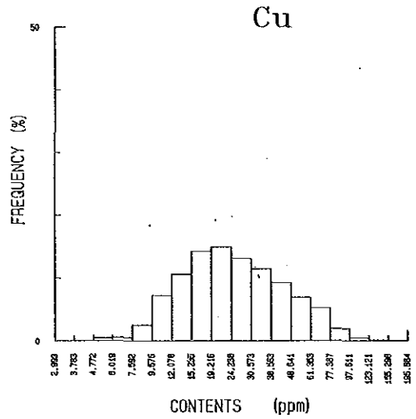

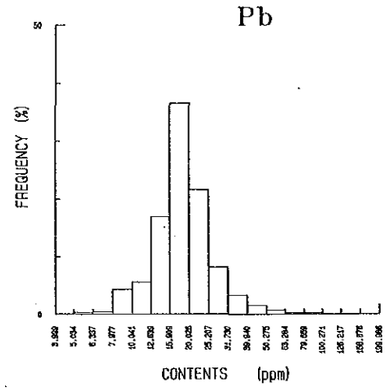

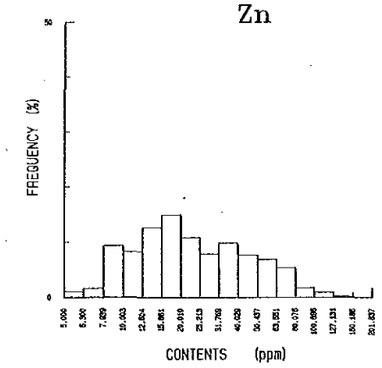

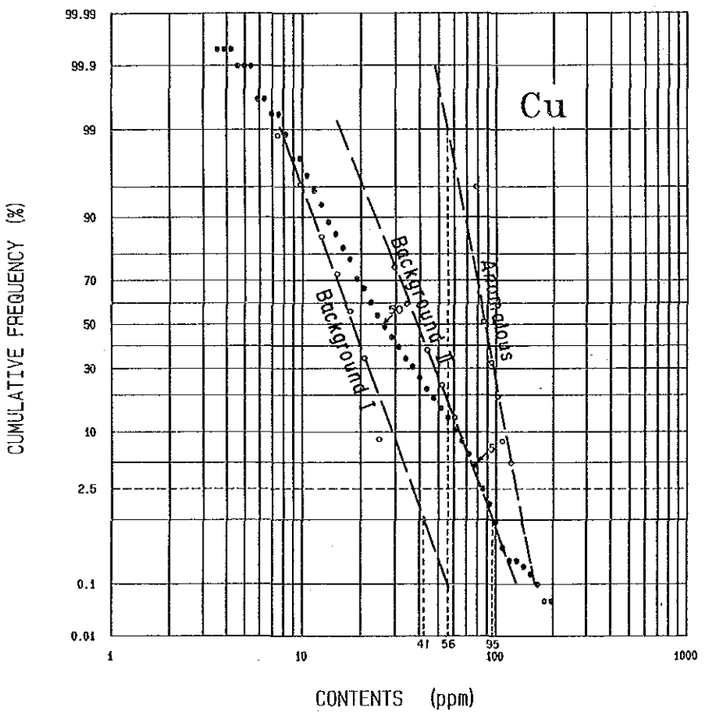

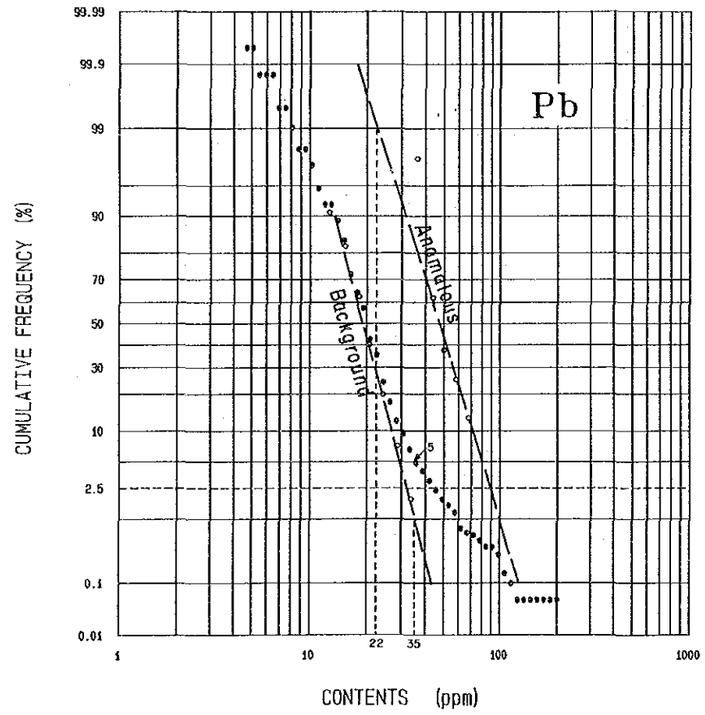

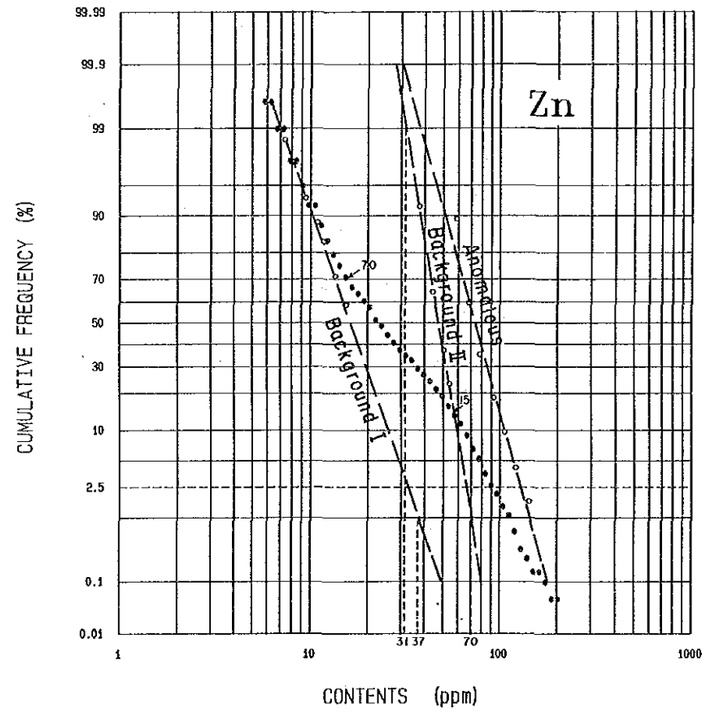

Fig. II-1-5 Histogram and Cumulative Frequency Distribution of Cu, Pb and Zn

Table II-1-2 Results of Simplified Statistical Treatment of Geochemical Data

	Values in ppm			Total data		Anomalous		Background (II)		Background (I)	
				%	No.	%	No.	%	No.	%	No.
Cu	Group I ≧ 95			1.7	35	26	26	1	9	-	-
	Group II ≧ 56			11.4	228	73	73	17	154	0.1	1
	Group III ≧ 41			11.3	227	1	1	24	217	0.9	9
	Group IV < 41			75.6	1,518	-	-	58	524	99.0	994
	Max	Min	Mean	100	2,008	100	100 (5%)	100	904 (45%)	100	1,004 (50%)
	196	3	25.1								
Pb	Group I ≧ 35			4.9	99	80	80			1	19
	Group II ≧ 22			26.6	534	19	19			27	515
	Group III < 22			68.5	1,375	1	1			72	1,374
	Max	Min	Mean	100	2,008	100	100 (5%)			100	1,908 (95%)
	200	4	18.6								
Zn	Group I ≧ 70			8.7	174	54	163	1.0	11	-	-
	Group II ≧ 37			56.8	1,141	45	136	90.5	999	1	6
	Group III ≧ 31			4.9	98	1	3	7.5	83	2	12
	Group IV < 31			29.6	595	-	-	1.0	11	97	584
	Max	Min	Mean	100	2,008	100	302 (15%)	100	1,104 (55%)	100	602 (30%)
	202	5	23.0								

Table II-1-3 Correlation Matrix of Three Elements of Geochemical Data

	Cu	Pb	Zn
Cu	1.000		
Pb	0.350	1.000	
Zn	0.713	0.211	1.000

Table II-1-4 Results of Factor Analysis of Geochemical Data

Factor Loadings (varimax rotation)			Communality
	Factor 1	Factor 2	
Cu	0.720	0.462	0.7315
Pb	0.098	0.587	0.3539
Zn	0.819	0.234	0.7255
Factor contributions	87.671%	14.291%	

1–2–2 Geophysical Survey

(1) Data Processing and Analysis

Raw data acquired at the field were collected into GDP-12 (data processor) in which raw data were transformed to apparent resistivities, phase-differences, magnitudes, 3-pt decoupled phase and P.F.E., and these raw and transformed data were stored in DR-1 (data recorder). These stored data are processed by HP9816S and/or HP9050 computer to present pseudosections, plan maps and various spectrum diagrams. The 2-D distributions of IP anomalous sources are estimated by means of the 2-D FEM model analysis taking into consideration of these pseudosections, plan maps, various spectrum diagrams and geological conditions. And the characteristics of the IP anomalous sources are studied by analysing spectral characteristics at each frequency range.

The illustrations made in this survey are listed below.

1) Apparent resistivity pseudosection (0.125 Hz)
2) Apparent resistivity plan map (0.125 Hz, n=1,3,5)
3) P.F.E. pseudosection (0.125 Hz – 1.0 Hz)
4) P.F.E. plan map (0.125 Hz – 1.0 Hz, n=1,3,5)
5) Phase-difference pseudosection (0.125 Hz)
6) 3-pt decoupled phase pseudosection (0.125 Hz – 0.375 Hz – 0.625 Hz)
7) Decoupled-phase pseudosection (3 Hz, 5 Hz, 8 Hz, 16 Hz, 32 Hz)
8) Cole-Cole diagram
9) Phase-difference spectrum diagram
10) Magnitude spectrum diagram
11) Integrated 2-D diagram

(2) Physical property

The physical property measurement is conducted generally in order to understand the physical property of rocks and/or layers distributed in the survey area. However, it is very difficult to measure it at the same natural condition at sampling site and the observed values acquired at the field are affected by the surrounding geology. Therefore, the values of physical properties measured do not necessarily coincide with the observed values at the field.

Rock samples are 31 pieces in total; 13 pieces are collected at the ground surface and 18 pieces are from the drilling cores.

Average values of resistivity and P.F.E. of all samples are 2,628 ohm-m and 2.34%, respectively. Within those samples, the average values of each drill-hole are as follows: at MBP-1 hole, 4,973 ohm-m and 1.55%; at MBP-2 hole, 3,716 ohm-m and 2.74%; at MBP-3 hole, 3,628 ohm-m

and 3.85%. Average resistivity values of three holes show almost the same values, but average P.F.E. value of the MBP-3 hole shows the highest.

Average resistivity and P.F.E. values of rock samples collected at the ground surface are 950 ohm-m and 1.6%, respectively, and show lower values than those of drilling cores. This lower values may be caused by strongly weathered rock samples, collected at the station 100W of Line 110S (110S-100W), 290S-145W, 350S-205W and 350S-250W. Average resistivity value except for rock samples collected at these locations, is 1,186 ohm-m.

The highest P.F.E. values are obtained from core samples at the depth of 114.45 – 114.50m and 149.95 – 150.00m of the MBP-2 hole, and at the depth of 111.95 – 112.00m of the MBP-3 hole.

1–2–3 Drilling Survey

(1) Identification of Drill Core and Selection of Samples for Testing and Chemical Analysis

Identification of drill core and selection of samples were carried out at the workshop of the CPRM camp.

Identification of drill core was made by semi-quantitative description of constituent minerals at depth of every 0.5 meter on the data sheets prepared at a scale of 1:100 for this purpose. The data were then compiled into a columnar section at a scale of 1 : 200 (see Fig. A–5). In parallel with the identification, photographs including close-up shots for the main showing of core, were taken for each two core boxes (about 7.5 m in length).

Selection of samples for testing and analysis was performed after completion of core identification of each hole.

Consideration was made for the samples for SIP physical properties measurement, thin sections, polished sections and ore analysis to take them in the adjacent sections so that the results of tests and analysis might readily be compared and investigated mutually.

The cores thus selected were split, and one half was stored while the other half was used for various tests and chemical analyses.

The numbers of selected samples for testing and analysis are sixteen for thin section, four for polished section and twenty for ore analysis.

All the samples selected for testing and analysis were brought back to Japan, where all the tests and analyses were made. The results of these tests and analyses are described in each related section of this report.

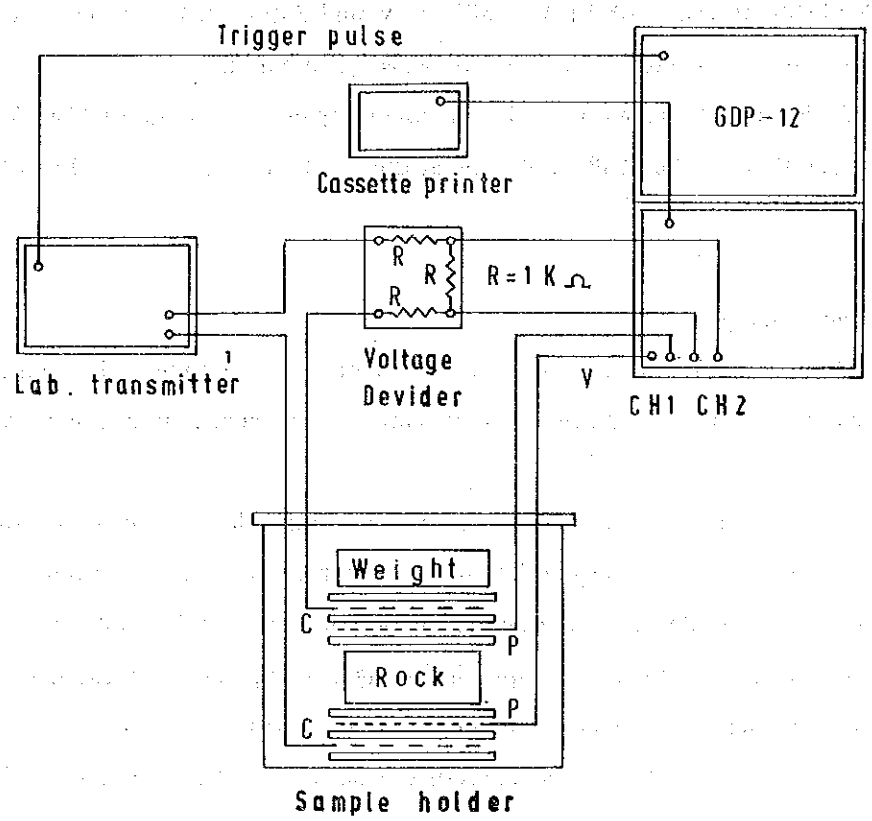

Fig. II-1-6 Brock Diagram for Sampling Measurements

Table II-1-5 Erectrical Property of Rock and Core Samples

試料採取位置	比抵抗（Ωm）	位相差(-mrad)	P.F.E.値(%)	備　　考
110S-130W	50	1.8	0.3	Quartzite
150S-235W	370	5.8	1.1	Amphybolite
270S-165W	497	18.6	2.5	Schist
270S-235W	4,490	12.8	1.8	Amphybolite
290S-145W	203	17.0	2.3	Schist
290S-245W	1,870	17.9	2.6	Quartzite
310S-165W	499	12.6	1.8	Schist
310S-176W	600	8.0	1.1	Schist
330S-252W	1,620	8.5	1.1	Amphybolite
330S-259W	855	12.5	1.7	Amphybolite
330S-165W	1,060	7.3	1.1	Schist
350S-280W	53	10.1	1.8	Schist
350S-205W	184	16.0	2.2	Schist
01- 34.45m- 35.50m	3,050	8.1	1.2	
87.50m- 87.55m	1,480	7.5	1.1	
194.00m-194.05m	7,170	18.1	2.8	
267.00m-267.05m	8,190	7.6	1.1	
02- 62.45m- 62.50m	1,860	3.1	0.5	
94.45m- 94.50m	9,310	15.8	2.3	
114.45m-114.50m	3,130	67.5	8.2	
149.95m-150.00m	6,770	36.2	5.2	
195.60m-195.65m	2,180	13.0	1.8	
233.20m-233.25m	1,790	10.3	1.5	
249.75m-249.80m	1,500	7.7	1.2	
289.50m-289.55m	3,190	7.4	1.2	
03- 39.95m- 40.00m	5,040	5.1	0.8	
111.95m-112.00m	351	188.1	17.8	
165.00m-165.05m	6,750	8.3	1.3	
185.50m-185.55m	1,610	4.1	0.6	
230.10m-230.15m	3,390	9.8	1.4	
290.00m-290.05m	4,630	9.9	1.2	

CHAPTER 2 Rio Dois de Junho Area

2–1 Results of Geological and Geochemical Surveys

2–1–1 Stratigraphy

Regional geology of the surrounding area of the Rio Dois de Junho area consists, from the base upward, of the Archaean Cana Brava basic-ultrabasic massif (Acb) which is the basement rock of the Project area, lower Proterozoic Palmeirópolis volcano-sedimentary Sequence (Pip), middle Proterozoic Serra da Mesa group (pmsm, Pm), Rio Maranhão cataclastic zone (ct), and upper Proterozoic Paranoá Group (Pspa).

Palmeirópolis volcano-sedimentary Sequence of these geology is distributed in the area as shown in Figures II–2–1 and II–2–2 and Plates II–2–1 and II–2–2. The Sequence is classified into five members, Pip_1, Pip_2, Pip_3, Pip_4 and Pip_5 (DNPM/CPRM, 1983), and shows the arrangement trending NE–SW ~ N–S.

(1) Pip_1 Member

Distribution

The member is the lower most geology in the area and distributed at the end of northeastern part on a small area.

Lithofacies

The rock is dark green, consisting of gabbroic coarse-grained amphibolite. The exposure of the fresh rock is limited to the areas along the rivers. The weathering parts become reddish brown fine-grained soil.

The result of microscopic observation of the typical rock is as follows:

Coarse - grained amphibolite (IH2021, Pip_1)

Locality : 796.70, 8532.12

Texture : Nematoblastic

Constituent minerals : hornblende > plagioclase ≫ quartz, opaque minerals, carbonate mineral, apatite, sericite, chlorite, epidote, K-feldspar, clay minerals.

Plagioclase is partly replaced by carbonate and clay minerals and sericite.

(2) Pip_2 vc Member

Distribution

The member is distributed on a very small scale in the northeastern and eastern limits. Several outcrops of the member were recognized in the northeastern limits in the current survey.

Lithofacies

The rocks are gray to brown lateritized schist containing muscovite, biotite, feldspar and quartz. Grains of garnet were recognized in the eastern limits.

Granitic rocks are found in parts of the northeastern limits where the floating stones consist of pegmatite locally.

(3) Pip_3 Member

Distribution

The member shows a form of two zonal arrangements from northeastern to eastern part and from north to southwestern part.

Lithofacies

The rocks consist mainly of dark greenish gray fine-grained compact amphibole schist. There is a banded texture consisting of leucocratic part with quartz – plagioclase and containing melanocratic part of amphibole, and/or lenticular quartz near the Pip_4 vs member locally. The member is intercalated with quartzite (qt), ferruginous quartzite (qtfe) and mica-quartz schist (xt).

The results of microscopic observation of the typical rocks are as follows :

Fine-grained amphibole schist (IH2003, Pip_3)

Locality : 792.46, 8532.19

Texture : nematoblastic

Constituent minerals : hornblende > plagioclase, sphene, carbonate minerals > epidote > quartz, opaque minerals > clay minerals

Mineral assemblage of hornblende – epidote can be seen.

Magnetite – quartz schist (VJ2008, qtfe)

Locality : 792.46, 8532.19

Texture : granoblastic, mozaic

Constituent minerals : quartz, opaque minerals.

Banded texture, consisting of coarse-grained quartz and fine-grained quartz – opaque minerals, is distinct. Arrangements of minerals and the direction of wavy extinction of quartz are oblique.

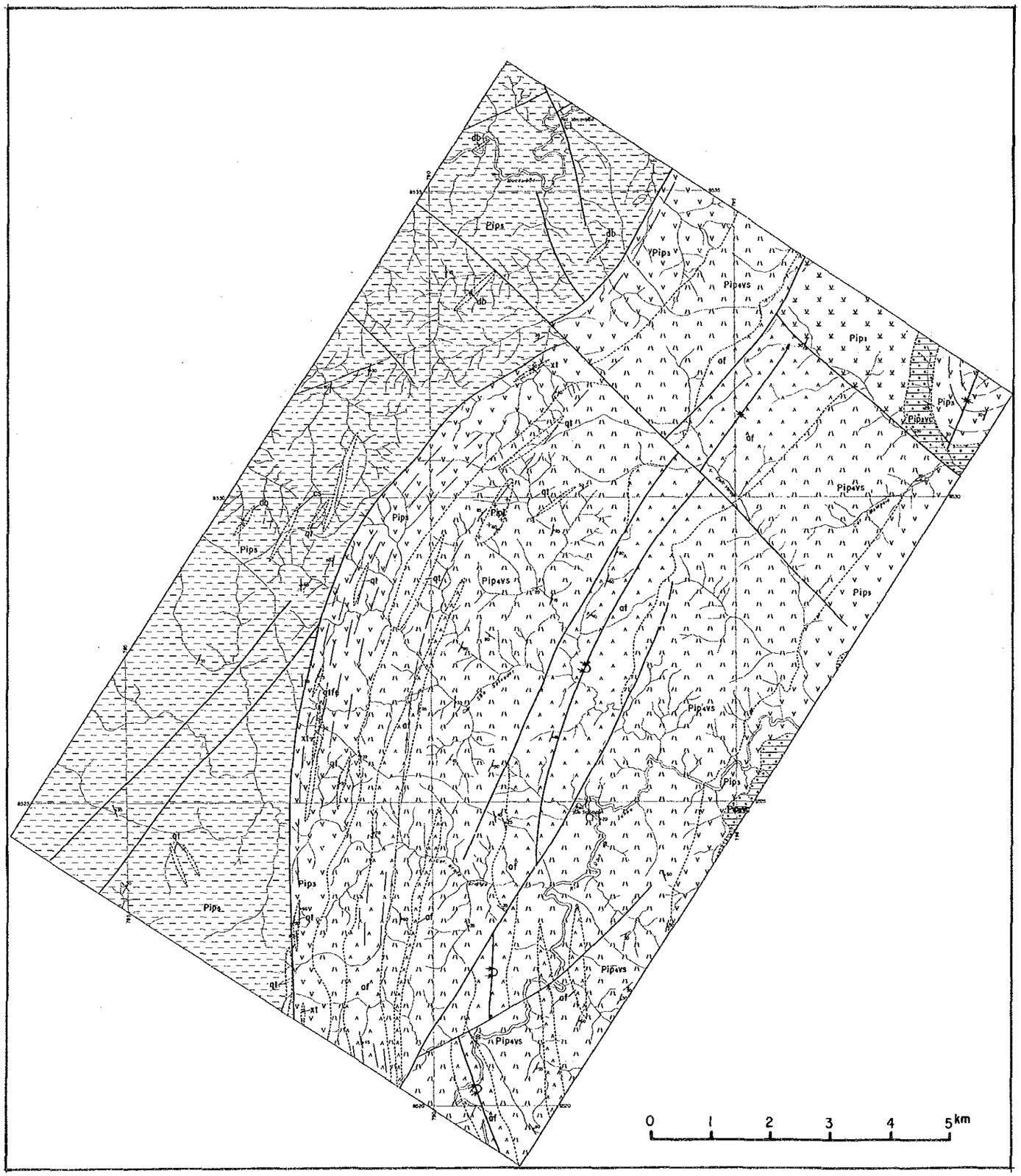

Paleoproterozoic Volcano - Sedimentary Sequence (RIBEIRO PENNO and TEIXEIRA, 1981)

Pip

- r : Filo granite (out of area)
- 5 : ste-bt-mv-qtz sch., ky-bt-mv-qtz sch., gnt-mv-qtz sch. and ky-ste-mv-qtz sch. associated with basic sill and dyke (db), banded iron formation (tf) and quartzite (qt) calc-silicate rock (cs)
- 4vxt : feldspathic gnt-bt-qtz sch (partly gneiss) and mica sch. including ky. and acidic meta tuff, with quartzite (qt) and amphibolite (af)
- r : granite, partly pegmatite (Morro do Acampamento Area)
- 4vxt$_3$ sc-mc-qtz sch. (rhyolitic composition)
- 4vxt$_2$: pl-mc-bt-qtz sch. and pl-bt-qtz sch. intercalated with amphibolite (af) (rhyolitic to rhyodacitic composition)
- 4vxt$_1$: feldspathic bt-qtz sch., ste-gnt-bt-qtz sch., bt-anf sch., biotitite and ck. rock (dacitic to rhyodacitic composition)
- 3 : dark fine-grained amphibolite with quartzite (qt), ferruginous quartzite (qtfe), gnt-bt-mv-qtz sch. (xt) and basic to ultra-basic dyke (db, ub)
- r : Morro Solto granite (out of area)
- 2gv : metagraywacke, metaconglomerate and ultrabasic sill (ub)
- 2vc : acidic to intermediate tuff, fapilli tuff, volcanic breccia and their schist
- 1 : gabbroic banded coarse-grained amphibolite

Zn-Cu-Pb showing

Lat. Ni ore

Zn-Cu-Pb ore

- Geological boundary
- Fault
- Synclinal axis
- Anticlinal axis
- 17° Bedding plane
- 25° Schistosity (S1)
- Schistosity (S2)
- 10° Lineation
- Lineament
- Gossan
- Sulphide dissemination

Fig. II-2-1 Geological Map of the Rio Dois de Junho Area

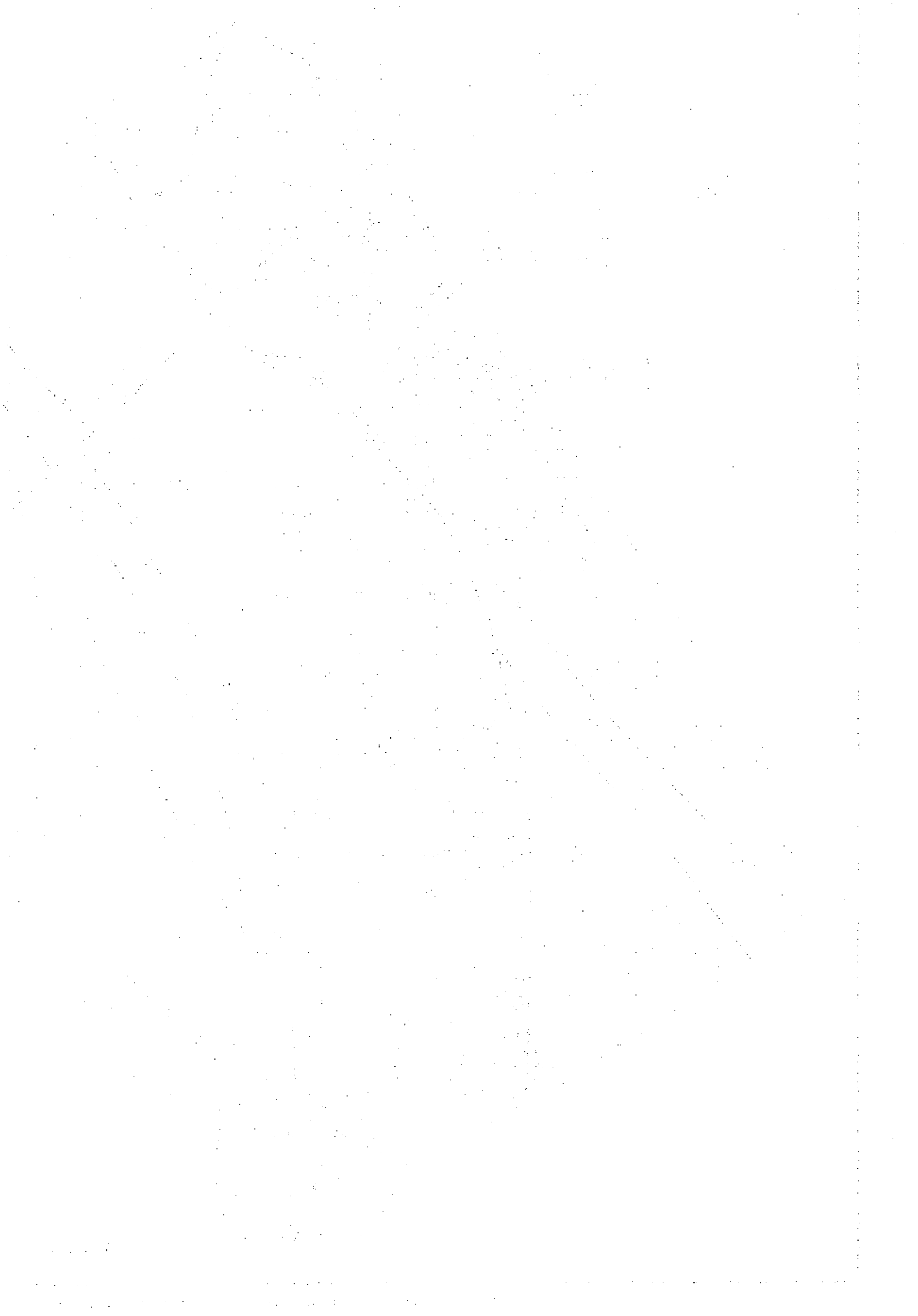

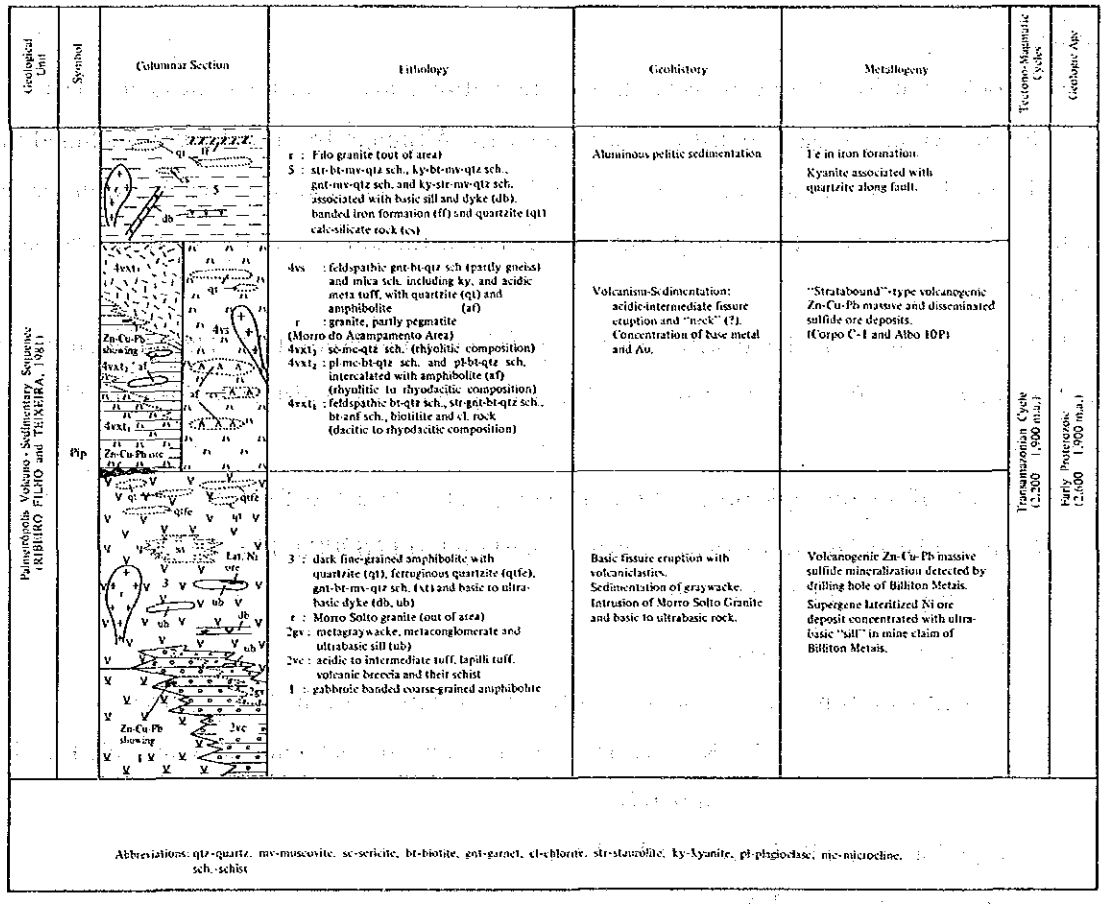

Fig. II-2-2 Generalized Stratigraphic Columnar Section in the Rio Dois de Junho Area

(4) Pip_4 vs Member

Distribution

The member is widely distributed from the northeastern to the southern parts occupying about half of the area.

Lithofacies

The rocks consist of gray feldspar-muscovite-biotite-quartz schist to gneiss in fresh part, and reddish brown mica-quartz schist in weathering part. Although fresh rocks were included into the granite (γ) because of the similarity of the lithology, the rocks showing banded structure are included into the gneiss at this time. Geological sketch of the outcrop in the southeastern part is shown in Fig. A–2.

The member is intercalated with quartzite (qt) and amphibolite (af). The latter shows the same lithology as the Pip_3 member and consists mainly of dark greenish gray fine-grained amphibole schist.

The results of microscopic observation of the typical rocks are as follows :

Garnet–plagioclase–muscovite–viotite–quartz schist (TS2008, Pip_4 vs)

Locality : 789.75, 8521.40

Texture : lepidoblastic

Constituent minerals : quartz > biotite, muscovite > plagioclase > garnet > K-feldspar, opaque minerals, sphene, sericite, zoicite, clay minerals

Fine-grained amphibole schist (IH2010, af)

Locality : 792.62, 8528.09

Texture : nematoblastic

Constituent minerals : hornblende > plagioclase, epidote ≫ quartz > opaque minerals, sericite, clay minerals

(5) Pip_5 Member

Distribution

The member is distributed from the north to the southwestern parts and widely occurs outside of the area.

Lithofacies

The rocks are composed of yellowish to reddish brown colored garnet–mica–quartz schist. Staurolite fragments of one centimeter in maximum length are observed in places 500m west from the boundaries with the Pip_3 member in the northwestern parts. The member is locally

intercalated with quartzite (qt) and light gray compact calc-silicate rocks (cs). The member is intruded by basic sills and dykes (db).

The results of microscopic observation of the typical rocks are as follows:

Staurolite–muscovite–quartz schist (VJ2019, Pip_5^s)

Locality : 790.50, 8532.94

Texture : lepidoblastic

Constituent minerals : quartz, muscovite > staurolite ≫ opaque minerals, andalusite > biotite

Carbonate–quartz rock (JR2001, cs)

Locality : 787.57, 8529.39

Texture : mozaic, banded

Constituent minerals : quartz > hornblende, carbonate minerals ≫ tremolite, sphene, zoicite, epidote.

Banded texture by the mineral arrangement consisting of coarse-grained quartz and fine-grained quartz–carbonitized hornblende is characteristic.

2–1–2 Intrusive Rocks

The intrusive rocks in the area are composed of granitic rocks (γ) and basic rocks (db).

(1) Granitic Rocks (γ)

Distribution

The rock is distributed in the central northern part trending in a NNE–SSW direction and having about 1.2km length with about 200m width.

Lithology

The rock is light gray and granoblastic muscovite–granite consisting of crystals of two millimeters in average diameter and is accompanied by muscovite–K-feldspar–quartz pegmatite containing crystals more than five millimeters locally. The rock includes some xenoliths of gneissose rocks which are similar to the fresh rocks of the Pip_4 vs member (Fig. A–3). The boundaries between granitic and gneissose rocks are unclear either in their field occurrences or under microscopic observation.

The results of microscopic observation of the typical rocks are as follows :

Muscovite granite (JR2008)

Locality : 790.89, 8529.58

Texture : granoblastic

Constituent minerals : quartz, K-feldspar > plagioclase, muscovite ≫ garnet, zoicite, epidole > sericite, clay minerals

Pegmatite / gneiss (NI2018)

Locality : 790.89, 8529.58

Texture : granoblastic/banded

Constituent minerals : pegmatite; quartz > K-feldspar ≫ muscovite, epidote > opaque minerals

gneiss; quartz > plagioclase, biotite, muscovite ≫ K-feldspar, epidote > garnet, opaque minerals, sericite, zoicite

Time of intrusion

It is thought that the granite intruded in early to middle Proterozoic (JICA/MMAJ, 1986).

(2) Basic Rocks (db)

Distribution

The rocks occur slightly in the Pip_5 member.

Lithology

The rocks consist mainly of green to dark green colored coarse-grained amphibolite and locally contain fine-grained gabbro. The rocks are partly accompanied by sulphide – quartz veinlet and sulphide dissemination.

The result of microscopic observation of the typical rock is as follows:

Porphyroblastic coarse amphibolite (JR2005)

Locality : 786.95, 8529.62

Texture : porphyroblastic, nematoblastic

Constituent minerals : hornblende > plagioclase, epidote ≫ quartz, sphene > opaque minerals, apatite.

Large crystals of hornblend cut the nematoblastic texture displayed by fine minerals.

2–1–3 Metamorphism

Metamorphic grade is assumed as follows based on the results of the field and microscopic observations.

Pip_1 and Pip_3 members (amphibolites) belong to epidote–amphibolite facies ~ amphibolite facies, and Pip_2, Pip_4 and Pip_5 members belong to garnet zone ~ staurolite–andalusite zone.

2–1–4 Geologic Structure

Because of bad condition of outcrop and developing area of schistose rocks, no bedding planes of the original rocks are recognized. And consequently, according to the distribution of rocks, strike and bedding of thin layers intercalated, characteristics of soil and photogeology, geologic structure of NE–SW system is distinct. Namely, the successions between Pip_3 and Pip_4 vs members are symmetrically distributed on the synclinal axis (partly overturned) at slightly east of the central part.

Fault systems of NE–SW and NW–SE directions are distinct. Compared with the sense of dislocation of horizontal component of both fault structures, the NE–SW system is right-lateral fault and the NW–SE system is left-lateral fault; therefore, these systems are considered to form a conjugate set.

The dominant direction of schistosity is almost parallel to the distribution of the members.

2–1–5 Mineralization

Two mineral showings, such as gossans on the boundary between Pip_4 vs and Pip_3 members in the eastern end and sulphide dissemination in the basic intrusive rocks of the northern part, are observed.

Some floats of gossans, having one meter in maximum diameter, consist of limonite with quartz networked veinlets and are scattered on an area of 50 meters in diameter. The assay result shows trace of Au · Ag, 0.00% of Cu · Pb and 0.01% Zn.

The sulphide minerals are recognized as dissemination and in quartz network veinlets in the basic intrusive rock. According to the microscopic observation, granular pyrrhotite dots the gangue minerals and shows the paragenesis with a small amount of chalcopyrite, magnetite and pentrandite. No small amount of Ti–minerals are also observed.

2–1–6 Results of Interpretation of Geochemical Survey

(1) Single Component Analysis

The anomalous values of each component obtained in the data processing stage were plotted on the drainage map (Fig. II–2–3 (above)).

In the first phase, the analysis was performed by lithofacies because content levels of each component were different in respective lithofacies (basic and schistose rocks). In the present phase, only the analysis of the entire samples was done because the contents levels were found more or less the same.

Copper (Cu)

The areas occupied by Group III (from 41 ppm up to below 56 ppm), including one percent of A population, 24% of B(II) population and 0.9% of B(I) population, are almost consistent with those of amphibolite. Group II (56 ppm or more and lower than 95 ppm), consisting of 73% of A population and 17% of B(II) population, is recognized in areas of high copper content in the areas distributed by amphibolite. With regard to Group I (95 ppm or more), which is composed of 26% of A population and one percent of B(II) population, five concentrated zones are extracted in the areas of amphibolite and another five in other areas.

Lead (Pb)

The areas underlain by Groups I and II are not consistent with the distribution of lithofacies. Group I (35 ppm or more) includes 80% of A population and 1% of B population, and Group II, 22 ppm or more and less than 35 ppm, includes 19% of A population and 27% of B population. As to the zones occupied by Group I, however, those in schistose rocks region rather than amphibolite region are extracted. Two concentrated zones were found in the Pip_4 vs member in slightly south of the central part.

Zinc (Zn)

Geochemical anomalous zones of Zn exhibit the same distribution as that of Cu anomalous zones. Namely, the areas of distribution of both Groups II and III almost correspond to those of amphibolite. Group II, 37 ppm or more and less than 70 ppm, includes 45% of A population, 90.5% of B(II) population and one percent of B(I) population. Group III, from 31 ppm up to below 37 ppm, consists of one percent of A population, includes 7.5% of B(II) population and two percent of B(I) population. The areas of Group I (70 ppm or more) which is composed of 54% of A population and one percent of B(II) population, are also included in the areas of amphibolite. But except in the areas of amphibolite, four areas of Group I were extracted.

(2) Multivariate Analysis

Figure II–4 (below) shows the analytical diagram of the first and second factors.

First Factor (Zn-Cu)

Based on the definitions that those with factor score of not less than 1.0 are the high factor score and those from 0.5 or more to less than 1.0 the moderate factor score, the zones of moderate to high factor scores were almost consistent with the areas underlain by amphibolite in the same way as the Cu and Zn anomalous zones extracted by the single component analysis.

The first factor is considered to reflect the characteristic of the country rock represented by amphibolite.

Second Factor (Pb-Cu-(Zn))

As the result of the analysis conducted in the same procedure as in the first factor, high factor score zones with those of 1.0 or more almost correspond to the area occupied by Group I of Pb.

Consequently, the factor might be related with the lead mineralization.

2–2 Discussion on the Results of Geological and Geochemical Surveys

Based upon the first order anomalous zones included in Group I of each element by the single component analysis and the high factor score zones of the second factor by the factor analysis, the investigation of relationship between these anomalous zones and mineralization resulted in extracting the important geochemically anomalous areas as shown in Fig. II–2–4.

As the areas which are included in the high factor score zones of the second factor as well as Group I of every component, two areas are extracted in the southern part. These two anomalous zone are distributed in the Pip_4 vs member, and the one on the south is of paticular interest in terms of its geological horizon as it is situated immediately above the Pip_3 member.

In addition, comparatively concentrated zones of geochemical anomaly except for those in amphibolite include the Pb zone in the Pip_4 vs member in slightly south of the central part and the Pb-Zn(-Cu) zone in the Pip_5 member in the west and southern-west parts.

No significant geochemical anomaly was obtained in the area overlain by gossan.

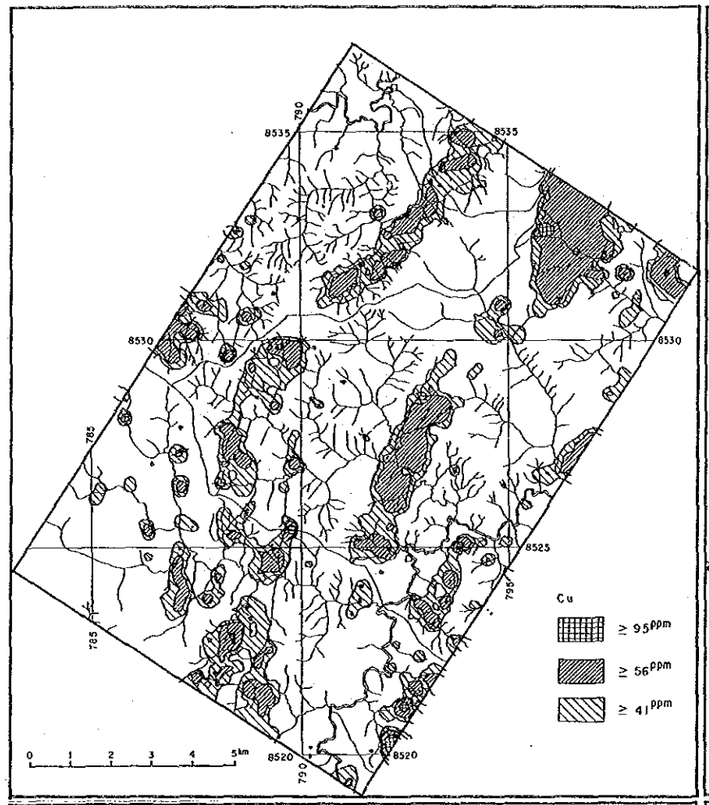

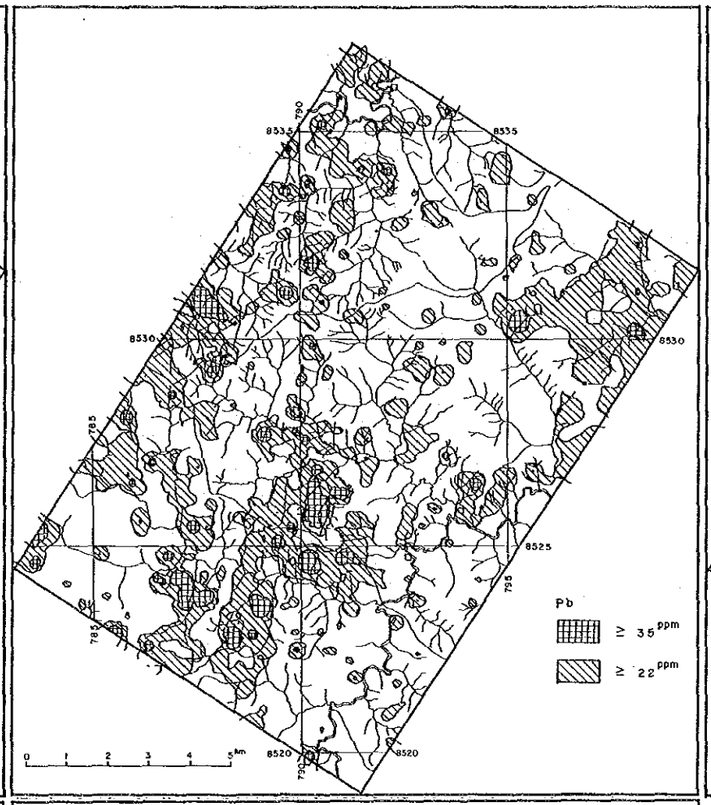

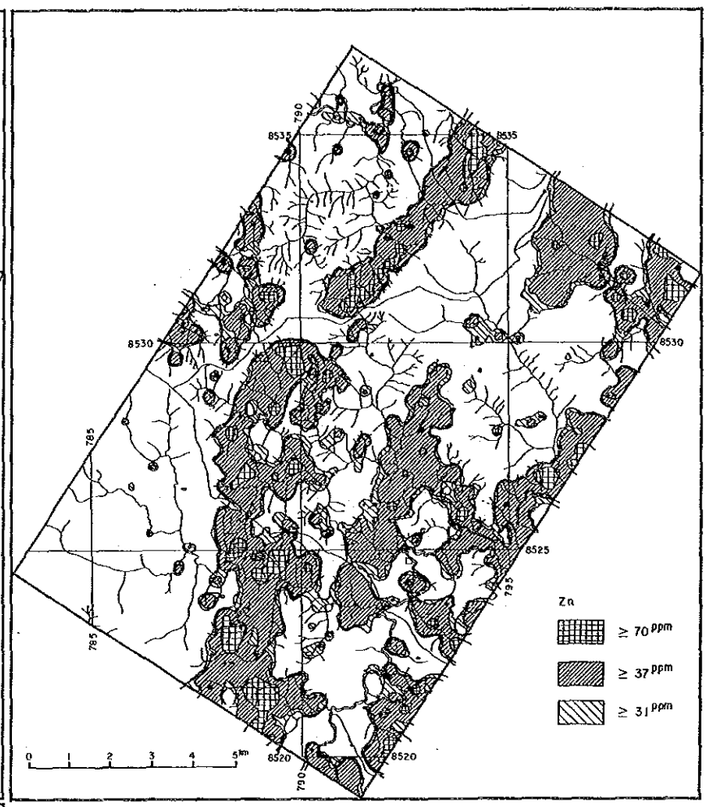

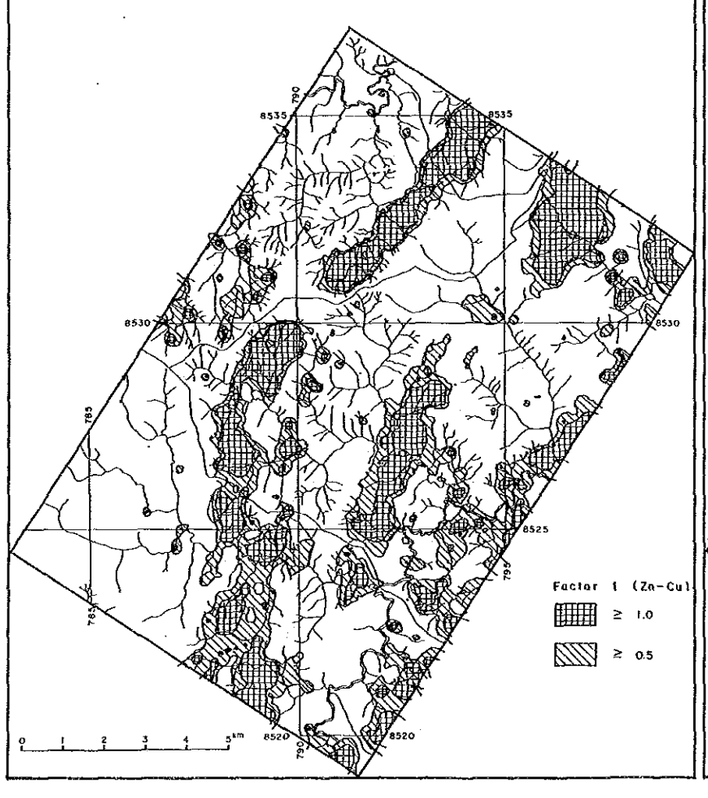

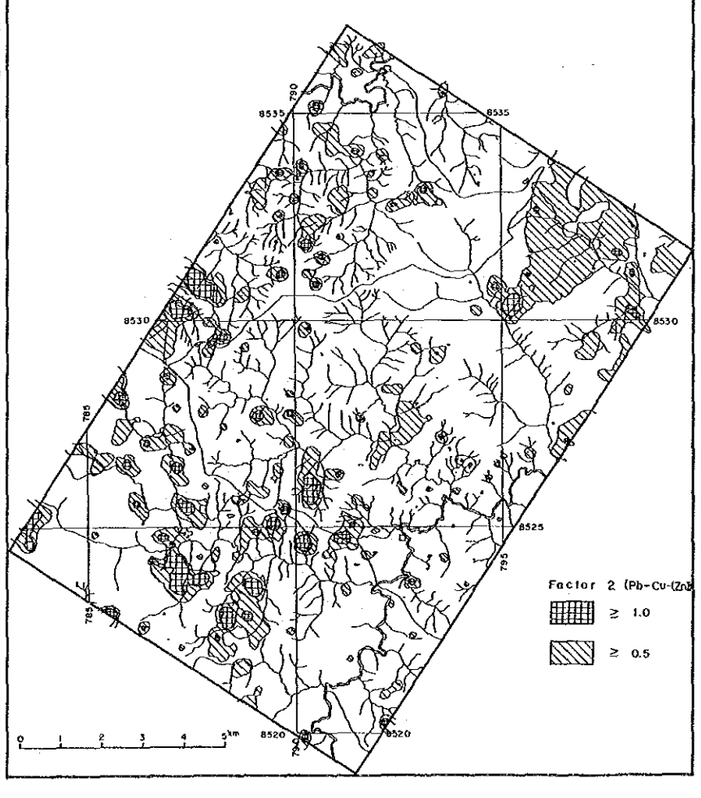

Fig. II-2-3 Geochemical Anomaly Map of the Cu, Pb and Zn and Factor Analysis Map of Geochemical Data

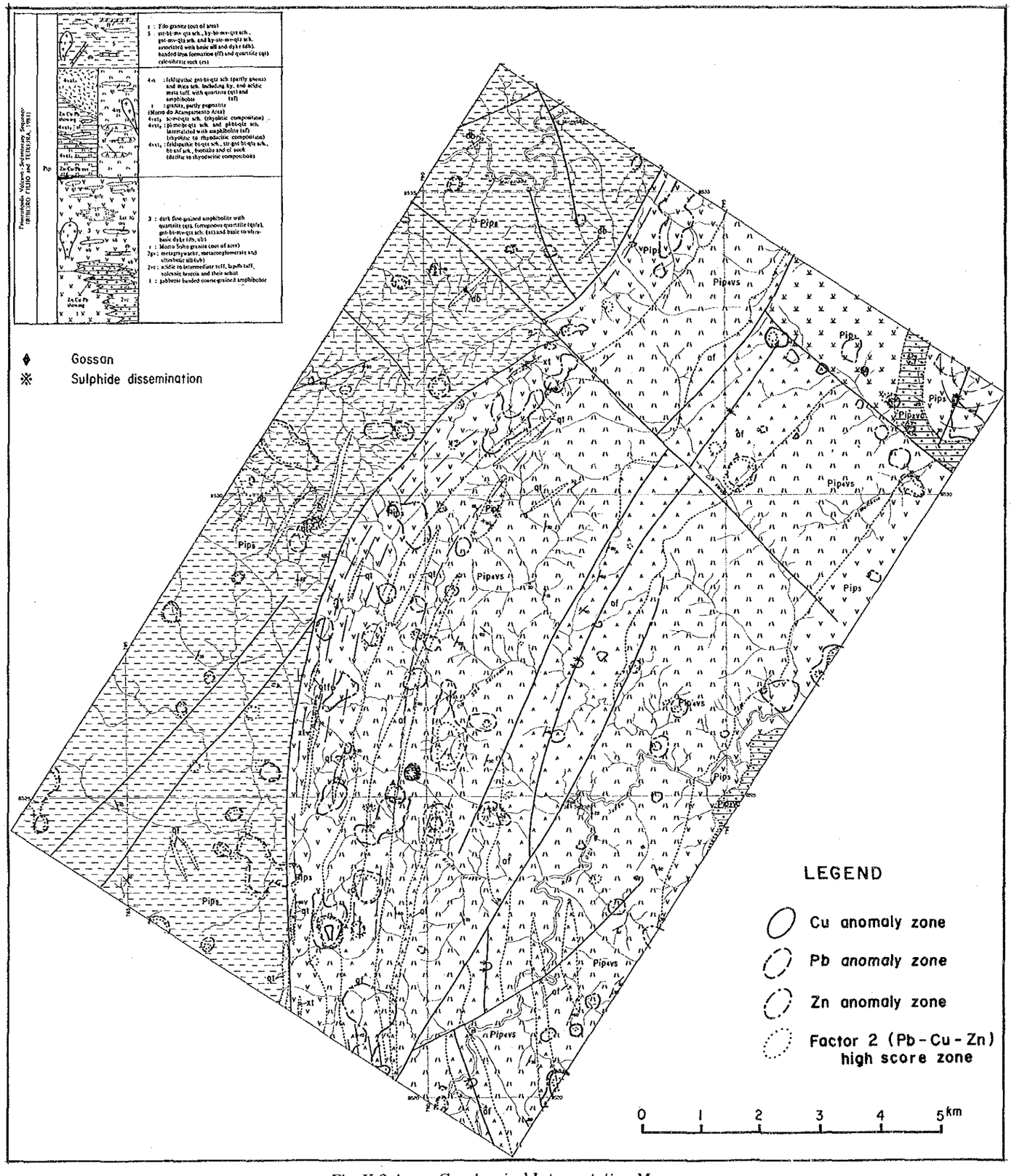

Fig. II-2-4 Geochemical Interpretation Map

Chapter 3 Morro do Acampamento Area

3–1 Results of Geophysical Survey

3–1–1 Pseudosections

SIP electrical survey was carried out in the Morro do Acampamento area, as a geophysical method of the second phase in the Palmeirópolis area. Taking into consideration of the results of geochemical and geophysical (CSAMT method) surveys in the last phase, SIP survey was applied in two blocks, "Block North" and "Block South", which are located at the northern and southern parts of the Morro do Acampamento. The direction of SIP survey lines is in NW-SE. Line 270S of the northern line of "Block South" was settled at 800m south of Line 190S of the southern line of "Block North".

Eleven SIP survey lines in total were set; 6 lines including one additional line (Line 160S, 800m in length) in the Block North and 5 lines in the Block South. Moreover, as the remarkable IP anomalies were detected at the west ends of Lines 270S and 310S at the Block South, those survey lines were extended to the west.

Interpretation results for each pseudosection are described as follows:

(1) Block North

Six survey lines, 110S, 130S, 150S, 160S, 170S and 190S, were set in this block. Within these, Lines 130S and 150S overlapped the survey lines in the last phase. And Line 160S was set to understand the southern extension of the IP anomaly detected at Line 150S.

1) Line 110S (Fig. II–3–1)

There may exist an insulating layer between stations 80W and 90W, so it was impossible to obtain deeper data at this portion.

Apparent resistivity section shows the strong resistivity contrasts reflecting the geology. Apparent resistivities higher than 1,000 ohm-m are distributed at the rectangular shape between 110W and 130W, surrounded by apparent resistivities of less than 500 ohm-m. A fault structure is assumed between stations 100W and 110W.

Background phase-difference values of larger than −10 mrad are predominant and there is no IP indication.

P.F.E. values of less than 2.0% are found on the whole section, but those of more than 2.0% are locally found at the depth between stations 130W and 150W, and at station 120W.

2) Line 130S (Fig. II–3–2)

There can be found strong contrast of apparent resistivities.

Apparent resistivities of higher than 1,000 ohm-m are distributed between stations 100W

and 130W, and between stations 130W and 150W. Those show a slightly west-dipping at the deeper part than n=2 at the former location and east-dipping from the ground surface of station 150W to the depth of station 130W at the latter location.

Apparent resistivities of less than 500 ohm-m are found near surface between stations 70W and 120W, and show east-dipping pattern between stations 130W and 160W.

Phase-differences lower than −20 mrad are found in the apparent resistivity zone of higher than 1,000 ohm-m between stations 100W and 130W.

P.F.E. values of higher than 2.0% are found between stations 80W and 120W, and at the west of station 130W, and distributed in the apparent resistivity zone of higher than 1,000 ohm-m.

3) Line 150S (Fig. II–3–3)

Apparent resistivities between 500 and 1,000 ohm-m are widely distributed.

Apparent resistivities of higher than 1,000 ohm-m are found in the depth between stations 110W and 150W, and those of lower than 500 ohm-m are distributed between sstations 90W and 100W, and between stations 110W and 120W.

Phase-difference of lower than −20 mrad are distributed from ground surface to the depth between stations 90W and 100W, and at the depth (n=5) at the west of station 100W. These distributions suggest the existence of east-dipping anomalous source.

P.F.E. values of higher than 2.0%, relfecting a strong IP anomaly, are distributed at the west of station 80W. Within these higher P.F.E. values, those of more than 3.0% suggest the existence of a strong IP anomalous source dipping to east, and are distributed in the apparent resistivity zone of higher than 1,000 ohm-m.

4) Line 160S (Fig. II–3–4)

Apparent resistivities of higher than 1,000 ohm-m are found in the depth between station 60W and 90W, and those of lower than 500 ohm-m are distributed at the depth of n=1 of the whole section.

Phase-difference of lower than −20 mrad are found in the apparent resistivity zone of higher than 1,000 ohm-m, and show the east-dipping distribution.

5) Line 170S (Fig. II–3–5)

Apparent resistivities of higher than 1,000 ohm-m are found in the depth between stations 80W and 60W and at the west of station 120W, and those of less than 500 ohm-m are distributed at the shallower part at the west of station 120W and at the east of station 100W.

Phase-difference of lower than −20 mrad are found at the depth of n=5 below station 80W

and in depth of n=4 between stations 110W and 150W and at station 100W. Those at station 80W and between stations 110W and 150W are distributed widely in the depth, but those at station 100W are seemed to be local.

P.F.E. values of higher than 3.0% show similar distribution as those of phase-difference of lower than −20 mrad.

6) Line 190S (Fig. II–3–6)

Apparent resistivities of higher than 1,000 ohm-m are distributed widely in the depth below n=2 at the west of station 120W, and in the depth at the east of station 80W extending to the east.

Phase-differences of −15 to −20 mrad are found on the whole section.

P.F.E. values of higher than 2.0% are found at station 90W, between stations 100W and 110W, at station 120W and between stations 140W and 170W. Those at the first two locations may be caused by east-dipping IP anomalous sources.

(2) Block South

In this block, five survey Lines, 270S, 290S, 310S, 330S and 350S, were set. Within these lines, as IP anomalies were detected at the western ends of Lines 270S and 310S, these two lines were extended to the west.

1) Line 270S (Fig. II–3–7)

Apparent resistivities show different distribution at the both sides of station 230W, where a fault structure and/or geological boundary may exist.

At the west of station 230W, those of lower than 500 ohm-m are distributed widely from the surface to the depth, but at the east those of higher than 1,000 ohm-m are found widely. And a low resistive layer may exist near the surface at station 280W.

On the phase-difference pseudosection, phase-difference of lower than −15 mrad are distributed at the east of station 220W and between stations 260W and 310W.

Those at the latter part are distributed in the apparent resistivity zone of less than 300 ohm-m, and show a strong IP indication dipping to east. On the P.F.E. pseudosection, the similar distribution pattern is found. And on the 3-pt decoupled phase pseudosection those are divided into two indications, shallow IP anomaly with low resistivity and high P.F.E. and deeper anomaly dipping to the east with medium resistivity and high P.F.E.

2) Line 290S (Fig. II–3–8)

Apparent resistivities show the different distributions between stations 210W and 220W, and near station 170W and near station 250W, respectively. Geological boundaries and/or fault structures are assumed at these three locations.

Apparent resistivities from 500 ohm-m to 1,000 ohm-m are found between stations 220W and 250W, and those of higher than 1,000 ohm-m are distributed between stations 160W and 220W.

Phase-differences of −20 mrad are found at the deeper part than n=2 at station 190W, showing west-dipping, and are distributed in the apparent resistivity zone of higher than 1,000 ohm-m. And in the apparent resistivity zone of lower than 1,000 ohm-m, phase-differences of higher than −15 mrad are dominated.

IP indications, on the 3-pt decoupled phase and P.F.E. pseudosections, show similar distribution patterns as those of phase-difference pseudosection. In particular, P.F.E. values of higher than 2.0% are distributed at deeper part than n=2 at station 190W, showing west-dipping.

3) Line 310S (Fig. II–3–9)

Apparent resistivities show a similar distribution as those of Line 290S.

At the west of station 240W, apparent resistivities of lower than 500 ohm-m are dominated and those of higher than 1,000 ohm-m are predominantly distributed in the depth between stations 240W and 170W. Therefore, the fault structure is assumed near station 240W.

Phase-differences of lower than −30 mrad, indicating a strong IP effect, are found between stations 270W and 280W, showing east-dipping, and distributed in the apparent resistivity zone of less than 300 ohm-m. And a weak IP indication of −15 to −20 mrad, found near station 220W, is distributed in the apparent resistivity zone of higher than 1,000 ohm-m, and is thought to be an extension from Line 290S. As distribution of IP indications on the 3-pt decoupled phase pseudosection are similar with those of phase-difference pseudosection, it is thought that there is little change of phase in the low frequency domain.

P.F.E. values of higher than 2.0% are found between stations 220W and 240W, and between stations 270W and 300W. Those at the former location may be caused by a weak IP anomalous source dipping to east. And those at the latter location show the distribution of IP indications reflecting two IP anomalous sources at shallower part and at the depth. Shallower source, showing west-dipping, is distributed in the apparent resistivity zone of less than 100 ohm-m. While, deeper one, showing east-dipping below n=2 at station 270W, is distributed in the apparent resistivity zone from 100 to 300 ohm-m.

4) Line 330S (Fig. II–3–10)

Apparent resistivities show different distributions at both sides of station 250W. At the west side of station 250W, apparent resistivities of less than 1,000 ohm-m decrease those value westward, and show the values of less than 200 ohm-m at station 270W. On the other hand, at the east side, apparent resistivities of higher than 1,000 ohm-m is distributed predominantly and

show higher values in the depth. A fault structure is inferred near station 250W.

A strong IP indication with phase-difference of lower than −30 mrad is found at station 280W and shows east-dipping. And a weak IP indication of phase-difference of −15 to −20 mrad, thought to be an extension form Line 310S, is distributed in the apparent resistivity zone of higher than 1,000 ohm-m.

P.F.E. values of higher than 2.0% are distributed on the whole line, and those distributions show similar pattern as those of phase-difference of lower than −15 mrad. P.F.E. values of higher than 4.0% at station 290W suggest the existence of a strong IP anomalous source, thought to be an extension from Line 310S.

5) Line 350S (Fig. II−3−11)

Apparent resistivities show different distributions at both sides of stations 270W − 280W. At the west side of station 280W, apparent resistivities of lower than 1,000 ohm-m are predominantly distributed and decrease those values westward. And at the east of station 270W, those of higher than 1,000 ohm-m are widely distributed. A fault structure is inferred between stations 270W and 280W, and this fault structure extends from Lines 290S, 310S and 330S in the direction of NNE-SSW.

The distribution of IP indications on the phase-difference and 3-points decoupled phase pseudosections show similar patterns of those of Line 330S. Phase-differences of lower than −15 mrad are found between stations 220W and 240W and at the west of station 270W. Those at the former location suggest the existence of a sheet-like and weak IP anomalous source near the surface, and those at the latter location may be caused by an east-dipping IP anomalous source from the surface to the depth.

3−1−2 Plan Maps

Plan maps for apparent resistivity and P.F.E. were made at depths of n=1, 3 and 5, which may reflect geological information at the depth of −100 mGL, −200 mGL and −300 mGL, respectively.

(1) Apparent resistivity plan map

Apparent resistivity plan maps, showing in Figs, II−3−12 to II−3−14, were made adopting terrain-corrected apparent resistivities.

Apparent resistivities in this area show distribution running in the N-S direction, and large variation reflecting the geological boundaries and/or fault structures.

1) n=1 (Fig. II−3−12)

At the Block North, apparent resistivities of lower than 1,000 ohm-m are dominated, and

LINE-110S

Apparent Resistivity (Ohm-m) [0.125Hz]

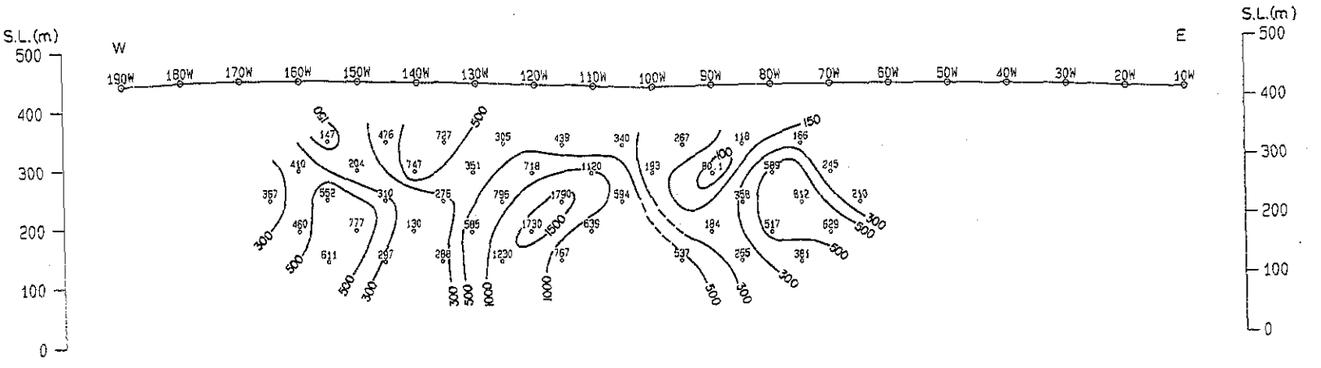

Raw Phase (-mrad) [0..125Hz]

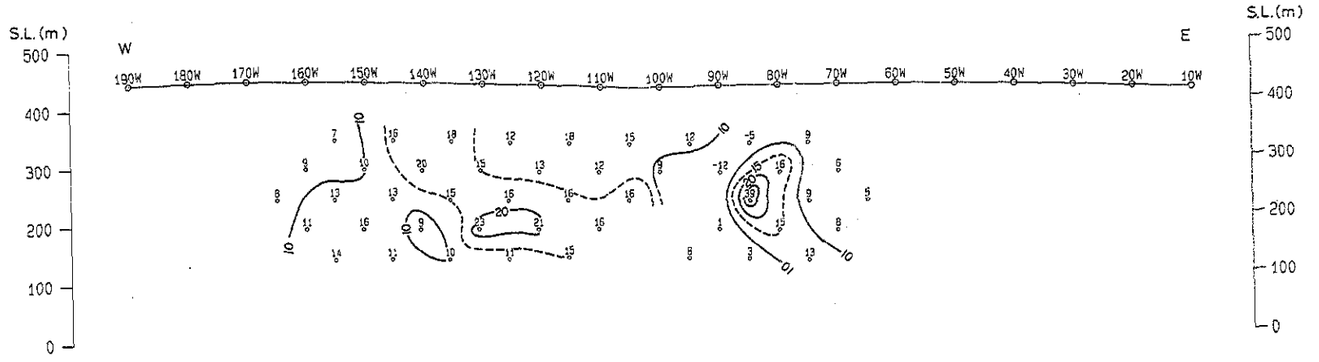

3-Point Decoupled Phase (-mrad) [0.125-0.375-0.625Hz]

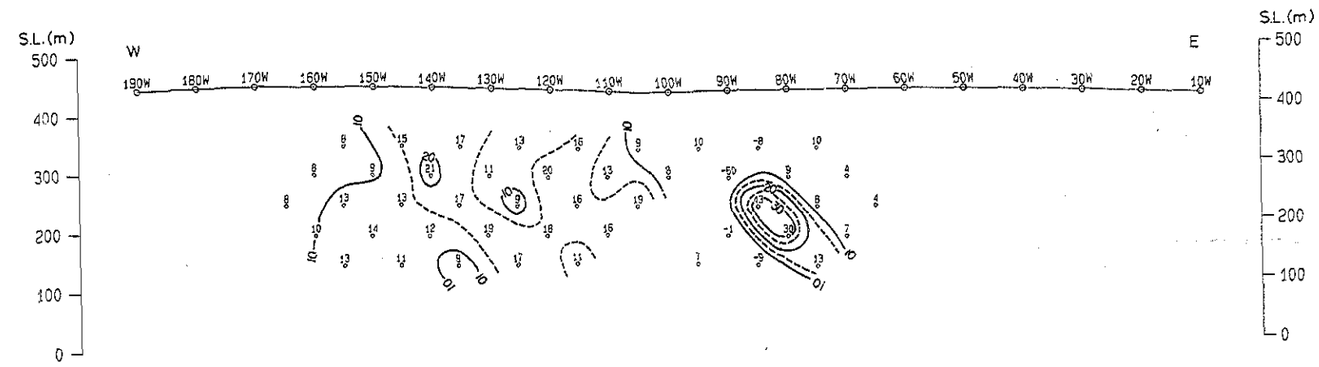

Percent Frequency Effect (%) [0.125-1.0Hz]

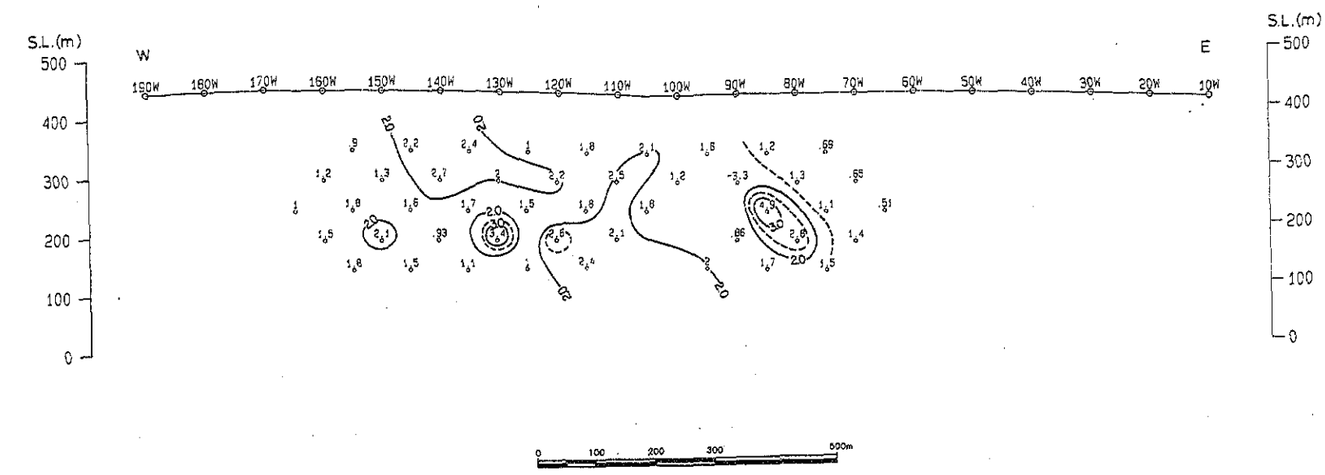

Fig. II-3-1 SIP Pseudo-Section (Line-110S)

LINE-130S

Apparent Resistivity (Ohm-m) [0.125Hz]

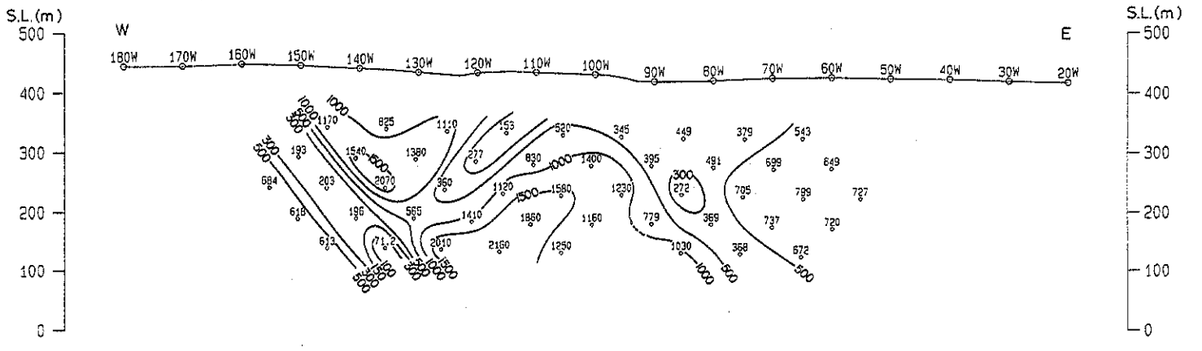

Raw Phase (-mrad) [0.125Hz]

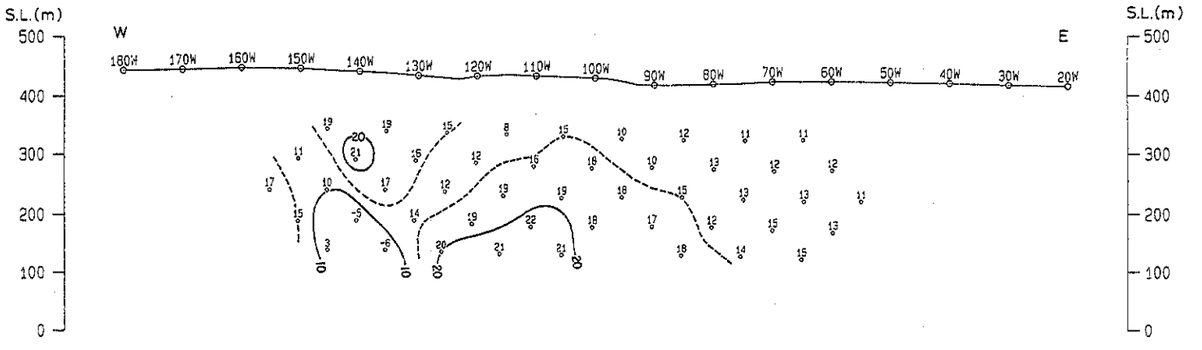

3-Point Decoupled Phase (-mrad) [0.125-0.375-0.625Hz]

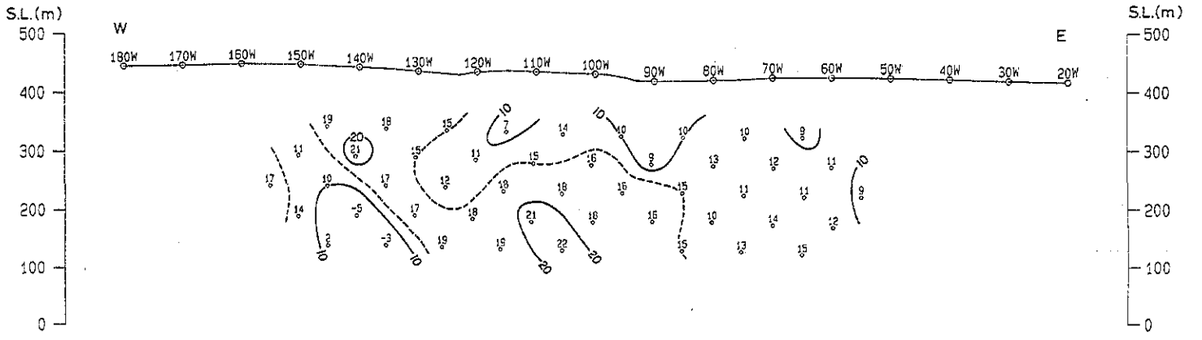

Percent Frequency Effect (%) [0.125-1.0Hz]

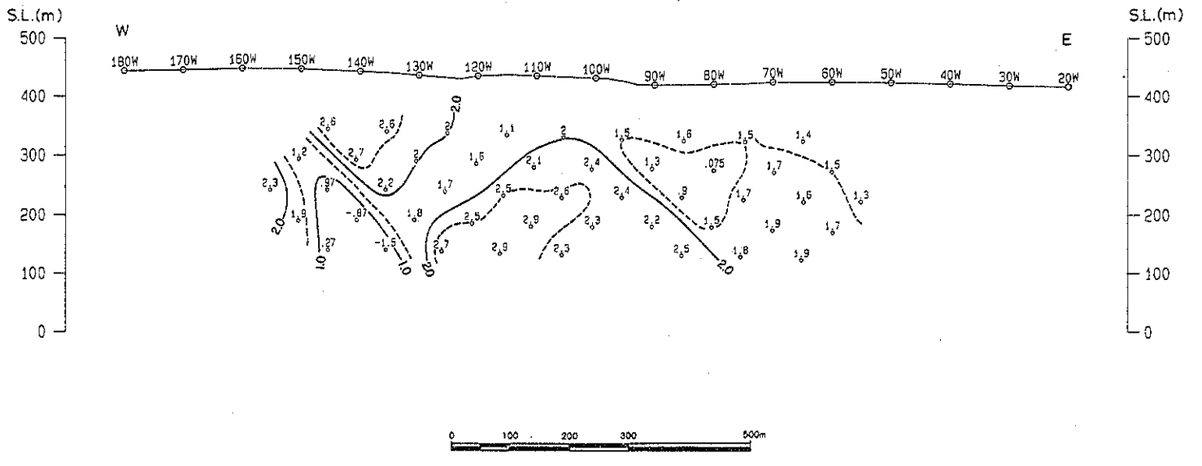

Fig. II-3-2 SIP Pseudo-Section (Line-130S)

LINE-150S

Apparent Resistivity (Ohm-m) [0.125Hz]

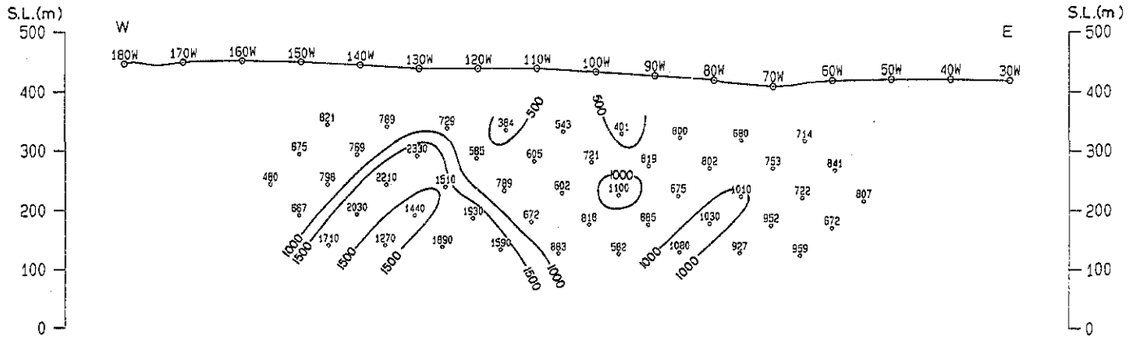

Raw Phase (-mrad) [0.125Hz]

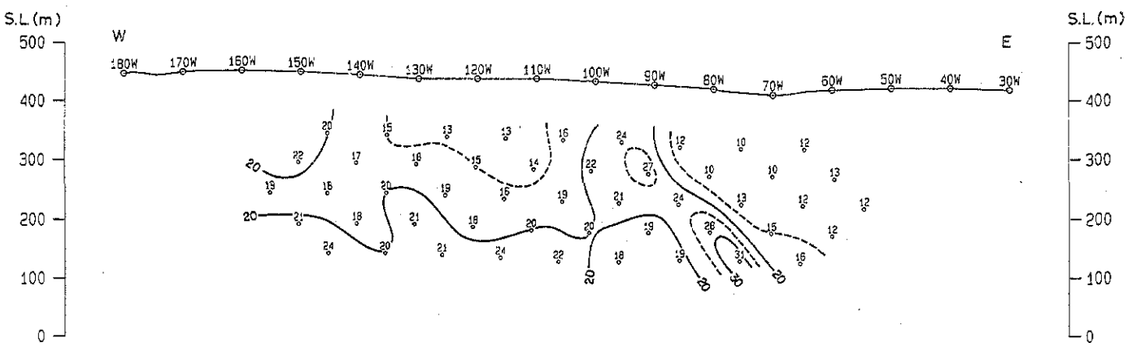

3-Point Decoupled Phase (-mrad) [0.125-0.375-0.625Hz]

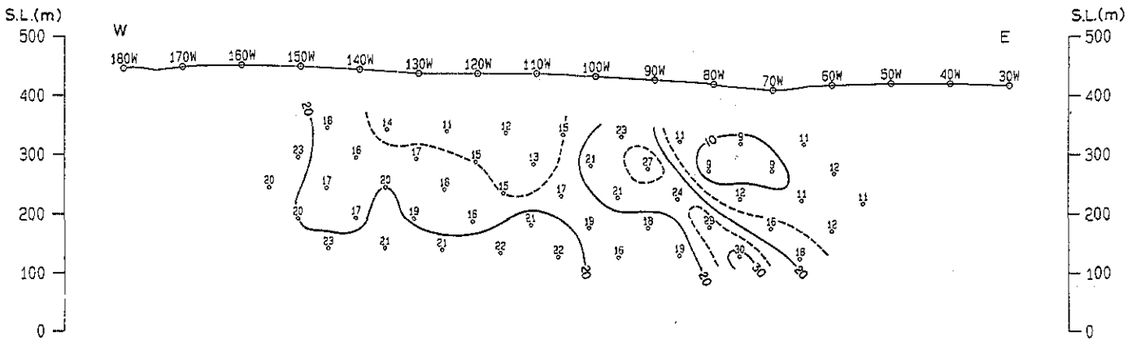

Percent Frequency Effect (%) [0.125-1.0Hz]

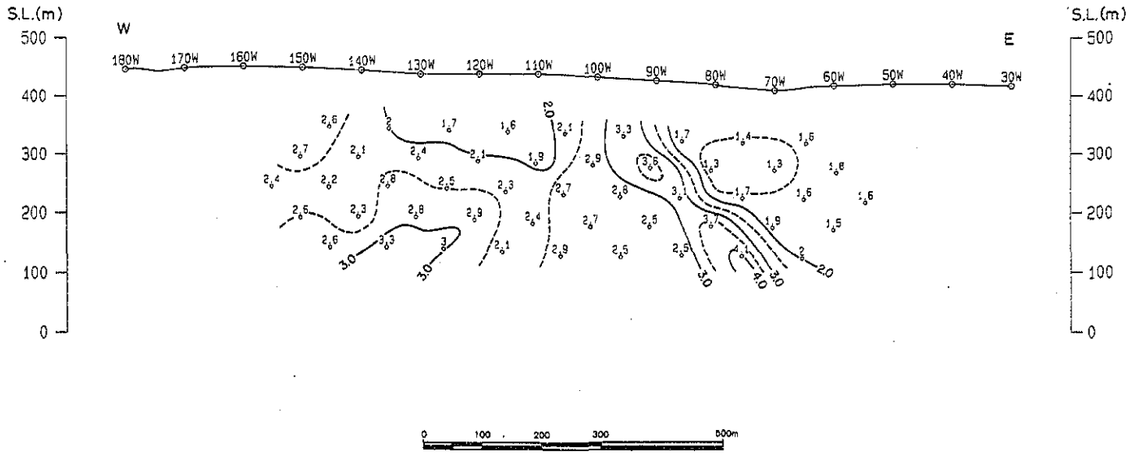

Fig. II-3-3 SIP Pseudo-Section (Line-150S)

LINE-160S

Apparent Resistivity (Ohm-m) [0.125Hz]

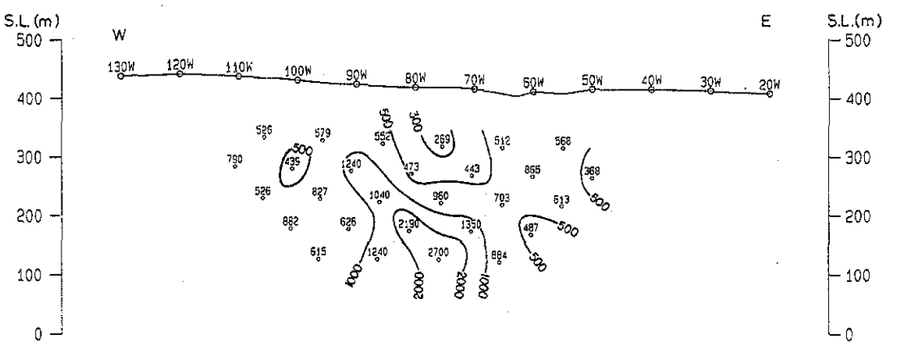

Raw Phase (-mrad) [0.125Hz]

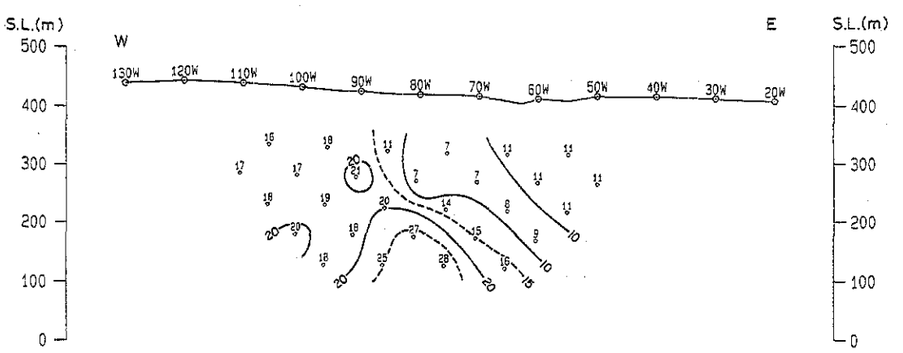

3-Point Decoupled Phase (-mrad) [0.125-0.375-0.625Hz]

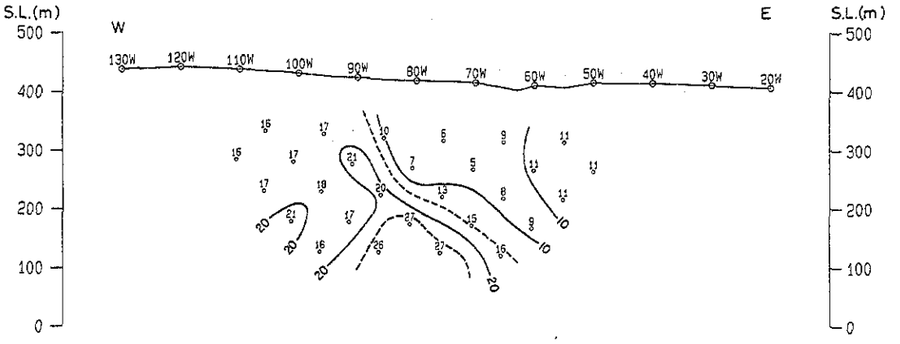

Percent Frequency Effect (%) [0.125-1.0Hz]

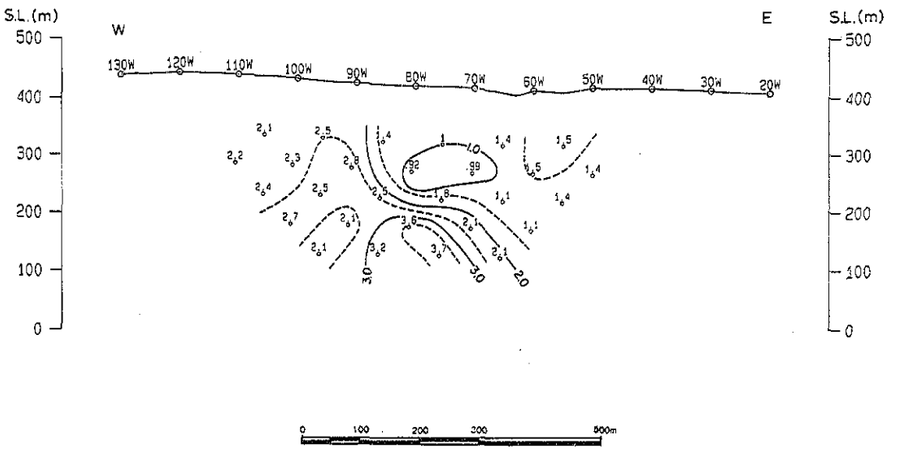

Fig. II-3-4 SIP Pseudo-Section (Line-160S)

LINE-170S

Apparent Resistivity (Ohm-m) [0.125Hz]

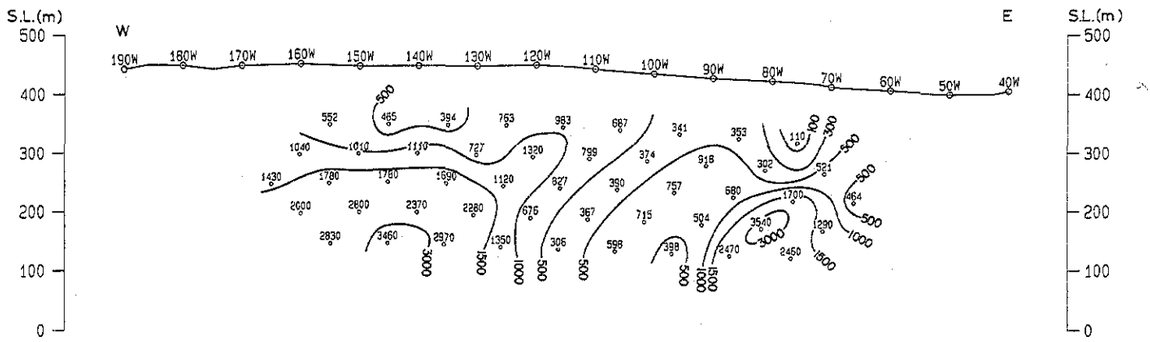

Raw Phase (-mrad) [0.125Hz]

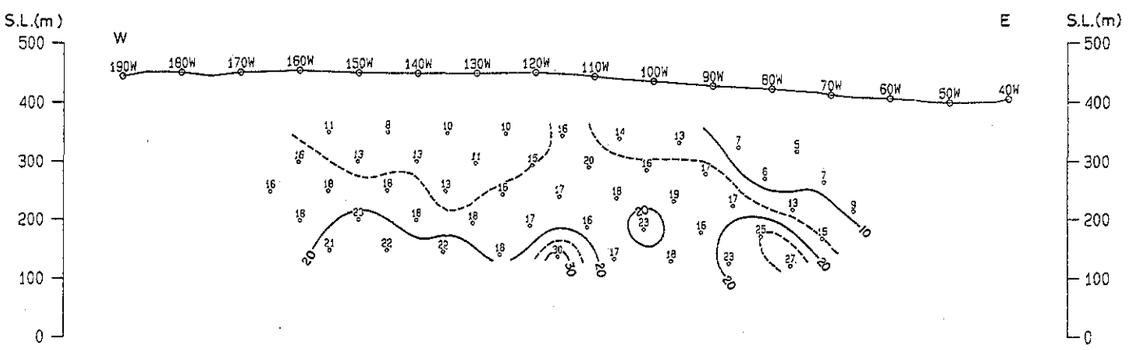

3-Point Decoupled Phase (-mrad) [0.125-0.375-0.625Hz]

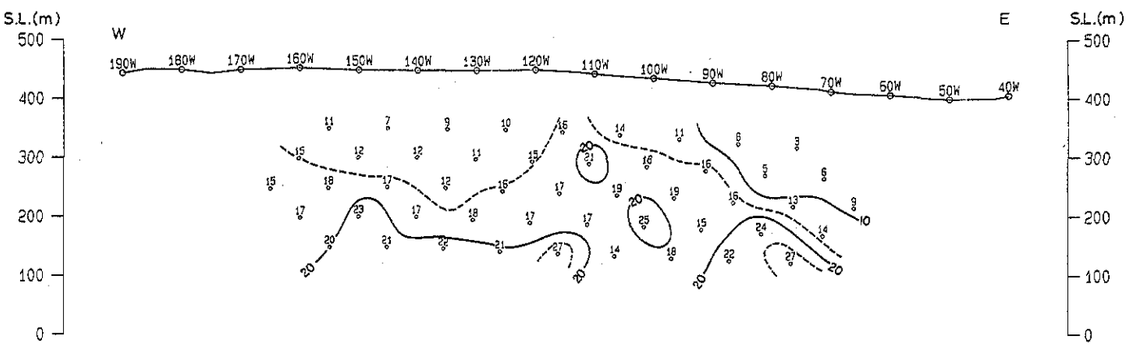

Percent Frequency Effect (%) [0.125-1.0Hz]

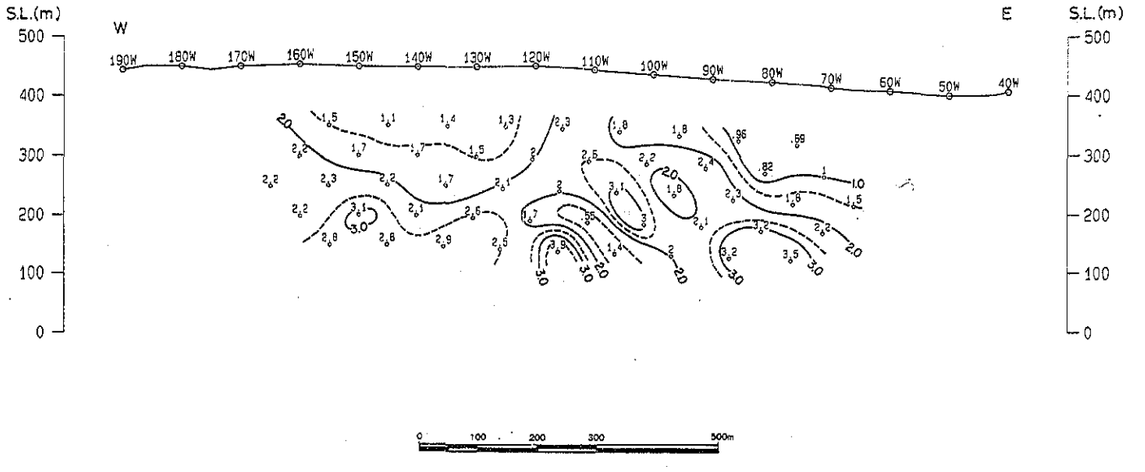

Fig. II-3-5 SIP Pseudo-Section (Line-170S)

LINE-190S

Apparent Resistivity (Ohm-m) [0.125Hz]

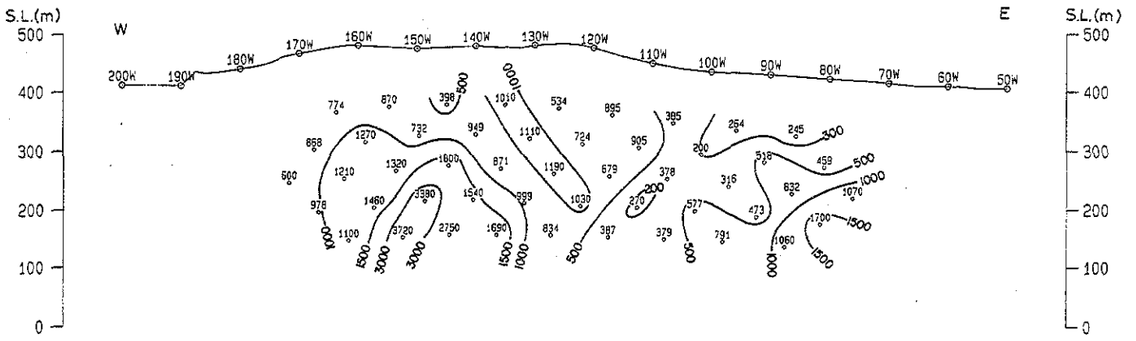

Raw Phase (-mrad) [0.125Hz]

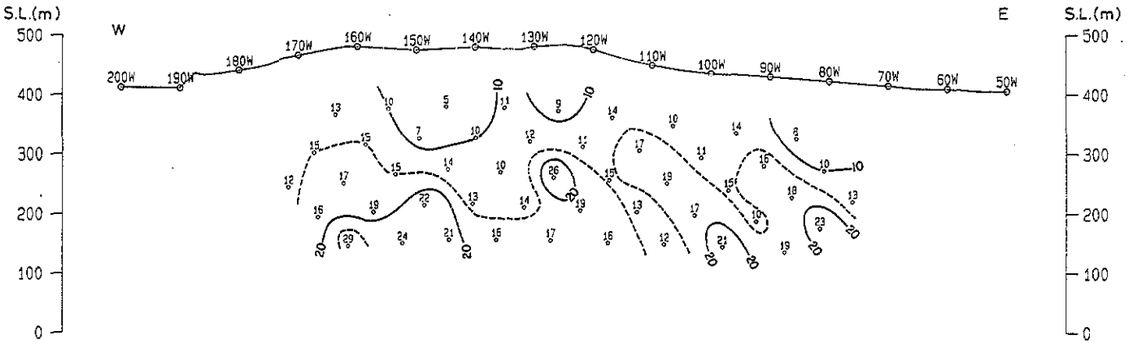

3-Point Decoupled Phase (-mrad) [0.125-0.375-0.625Hz]

Percent Frequency Effect (%) [0.125-1.0Hz]

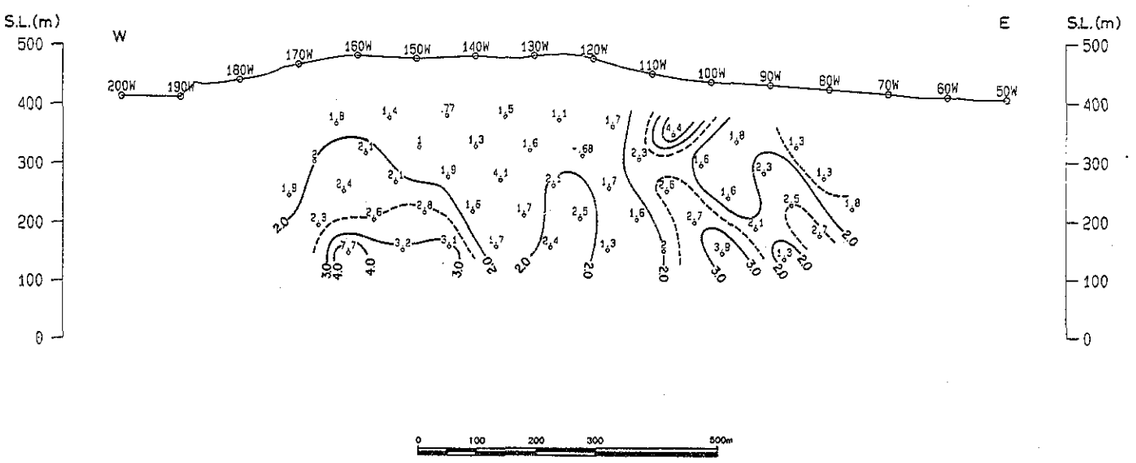

Fig. II-3-6 SIP Pseudo-Section (Line-190S)

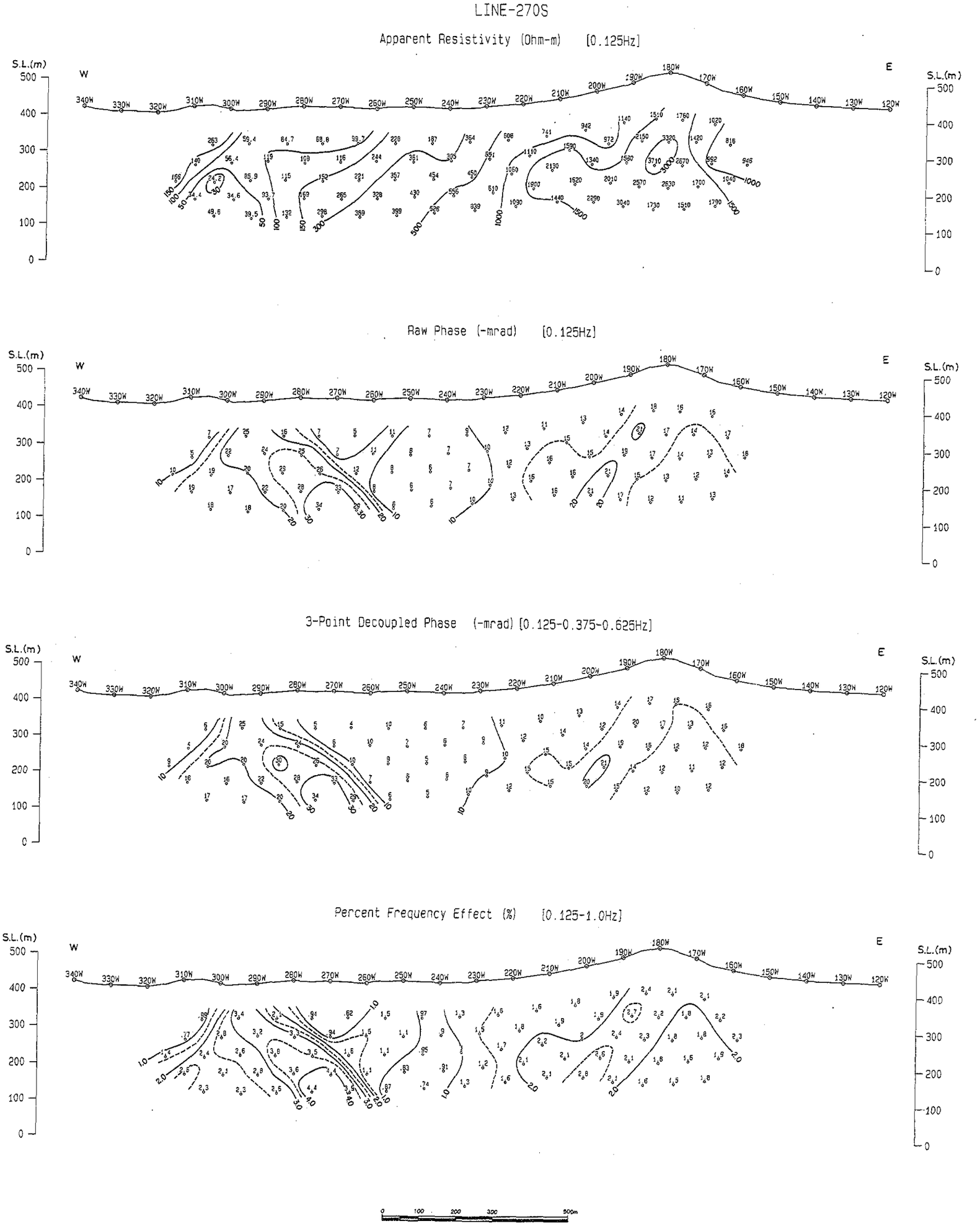

Fig. II-3-7 SIP Pseudo-Section (Line-270S)

LINE-290S

Apparent Resistivity (Ohm-m) [0.125Hz]

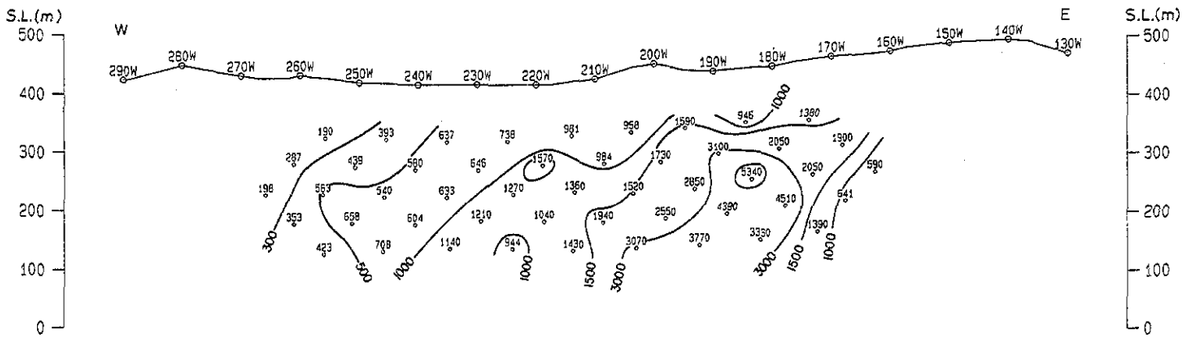

Raw Phase (-mrad) [0.125Hz]

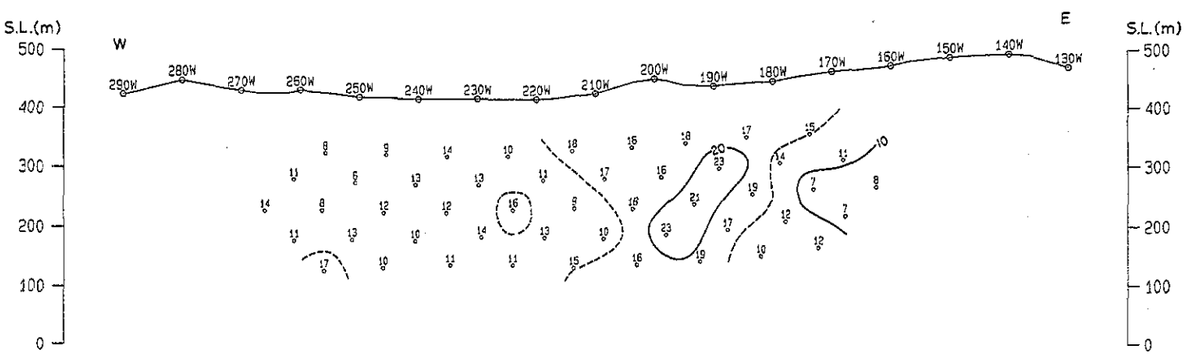

3-Point Decoupled Phase (-mrad) [0.125-0.375-0.625Hz]

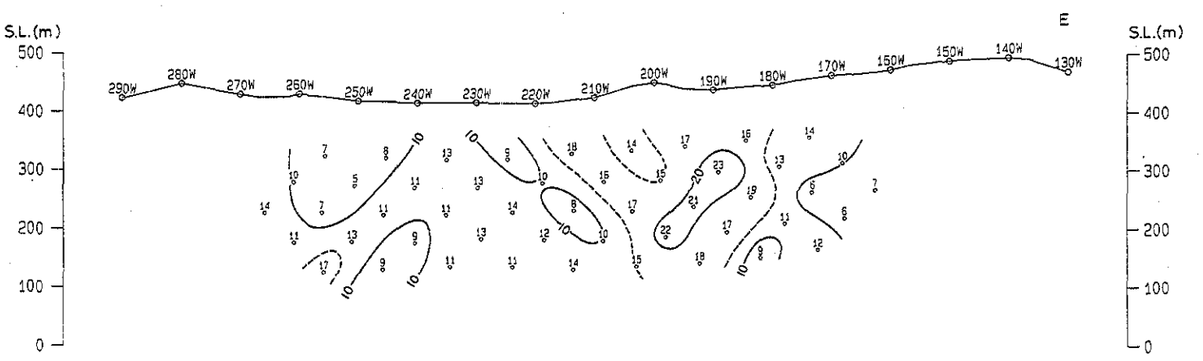

Percent Frequency Effect (%) [0.125-1.0Hz]

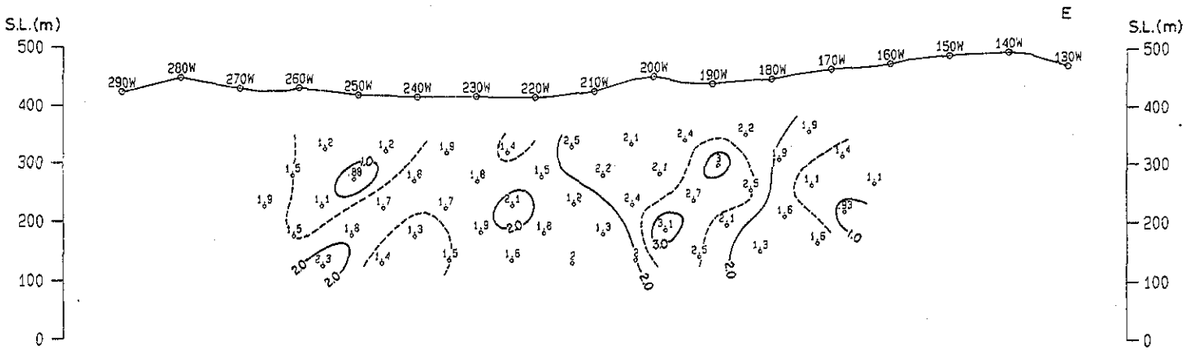

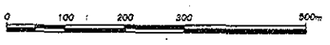

Fig. II-3-8 SIP Pseudo-Section (Line-290S)

LINE-310S

Apparent Resistivity (Ohm-m) [0.125Hz]

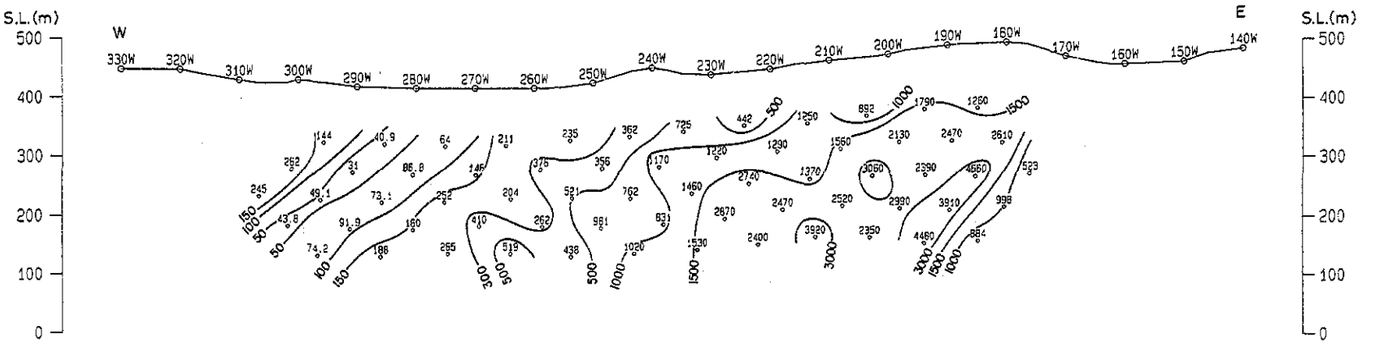

Raw Phase (-mrad) [0.125Hz]

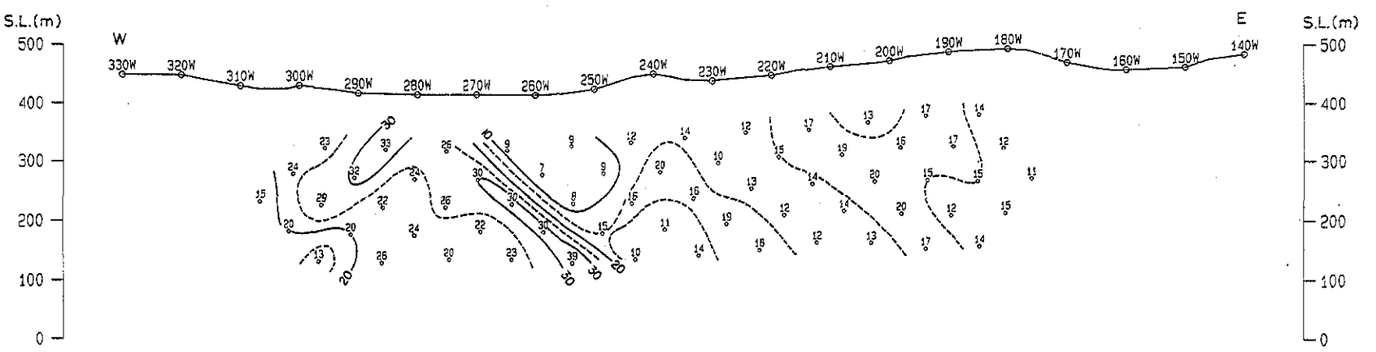

3-Point Decoupled Phase (-mrad) [0.125-0.375-0.625Hz]

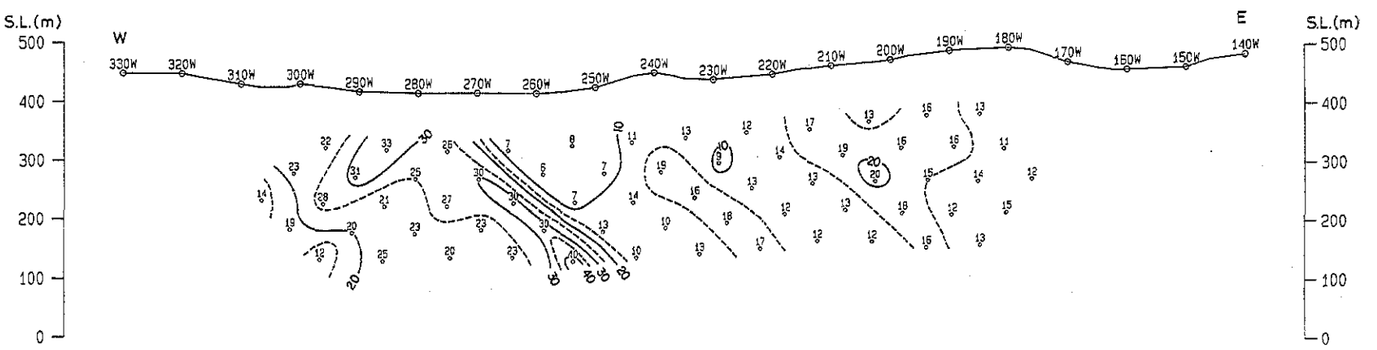

Percent Frequency Effect (%) [0.125-1.0Hz]

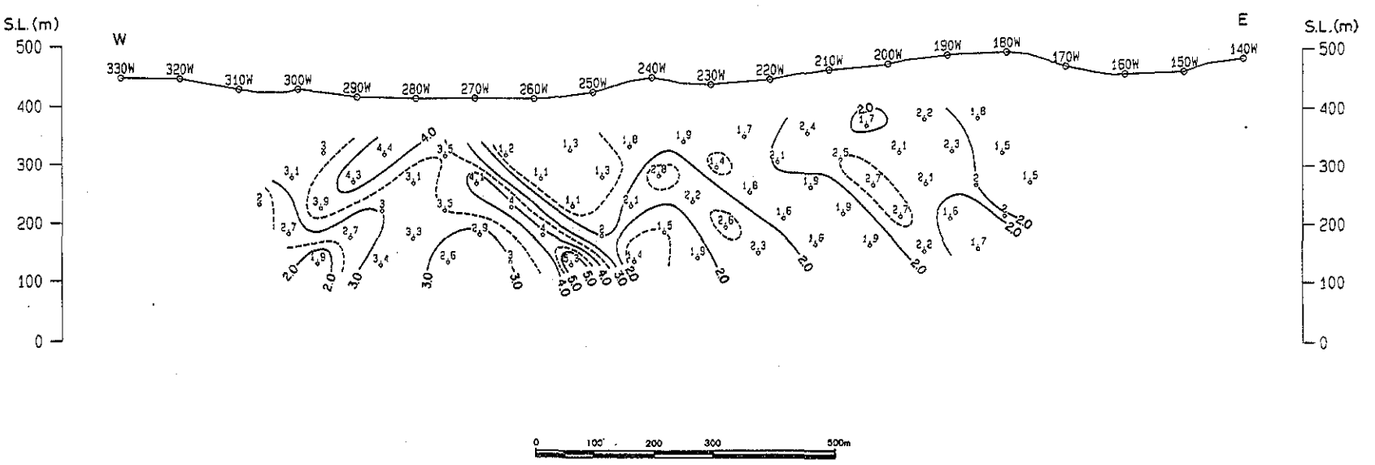

Fig. II-3-9 SIP Pseudo-Section (Line-310S)

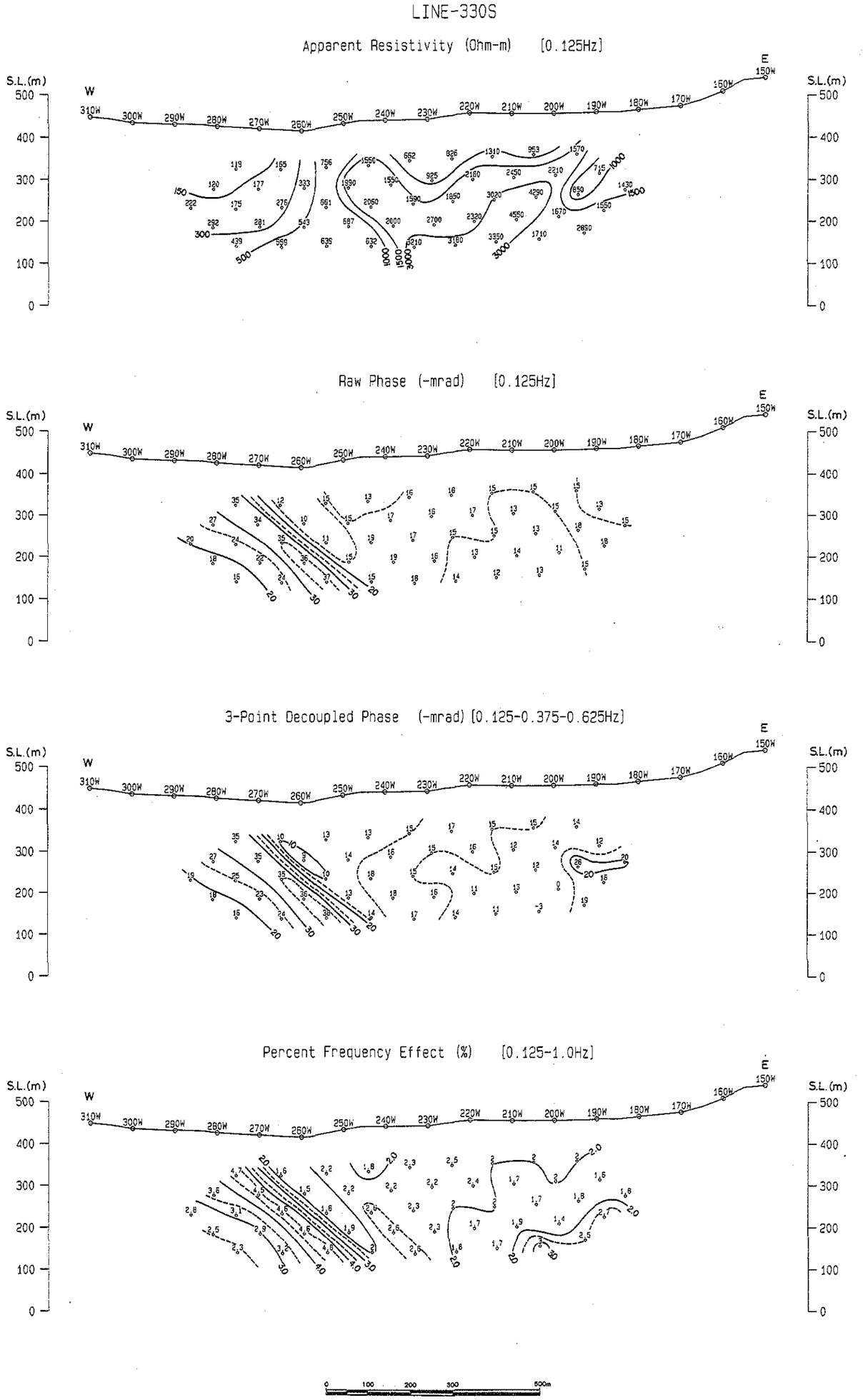

Fig. II-3-10 SIP Pseudo-Section (Line-330S)

LINE-350S

Apparent Resistivity (Ohm-m) [0.125Hz]

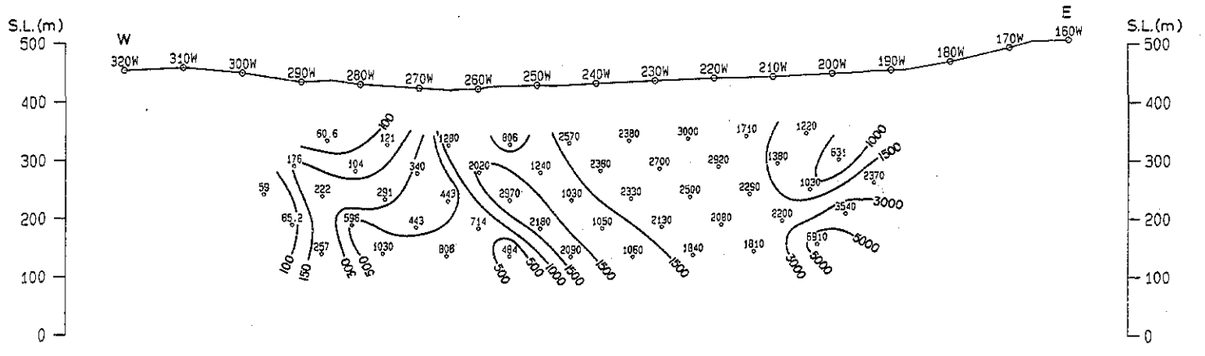

Raw Phase (-mrad) [0.125Hz]

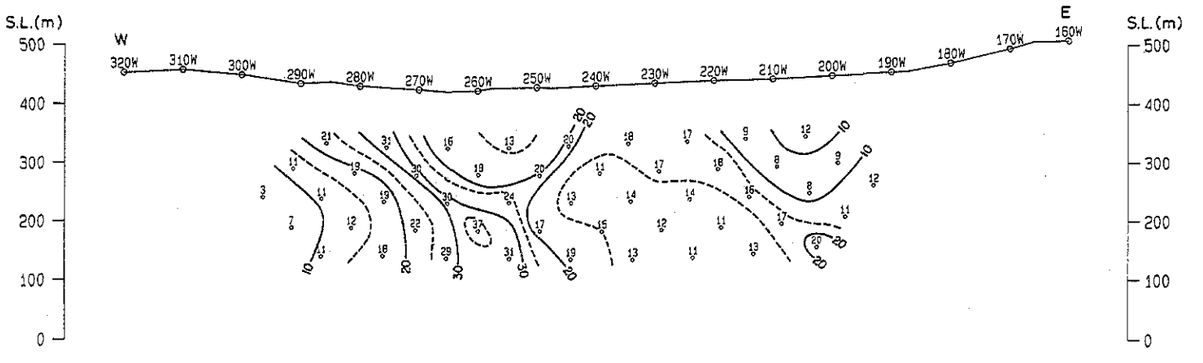

3-Point Decoupled Phase (-mrad) [0.125-0.375-0.625Hz]

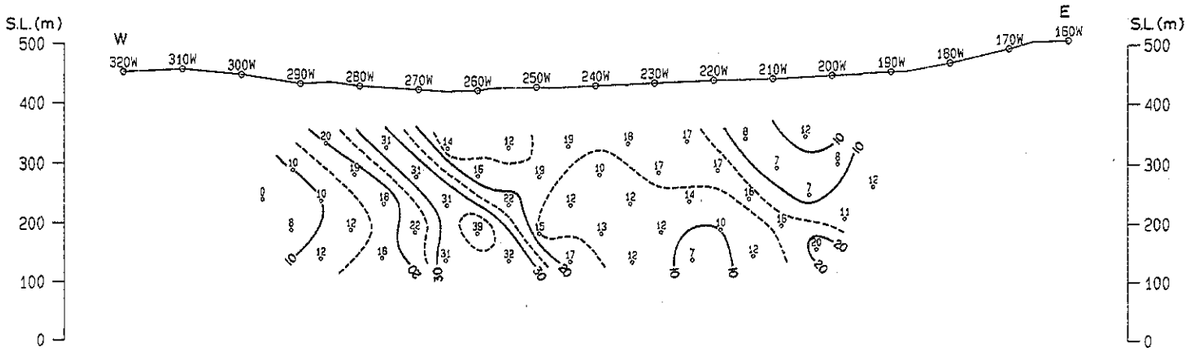

Percent Frequency Effect (%) [0.125-1.0Hz]

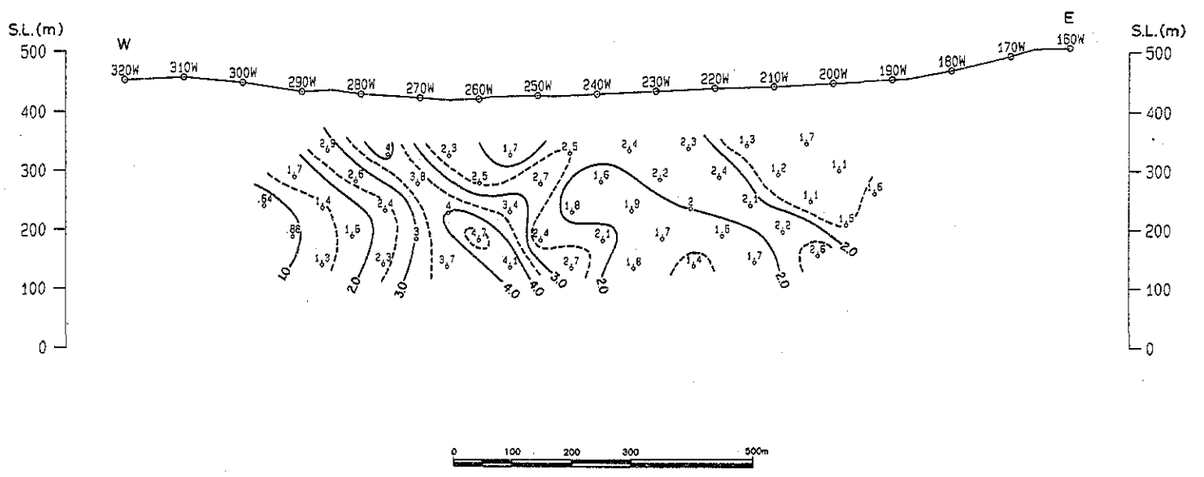

Fig. II-3-11 SIP Pseudo-Section (Line-350S)

those of higher than 1,000 ohm-m can be seen sparsely. Those of lower than 500 ohm-m are found independantly at the northern, southeastern, northwestern and southern parts, and those may extend to each direction beyond the block. And those of 500 to 1,000 ohm-m are distributed bloadly in the rest area.

At the Block South, apparent resistivities show a remarkable NNE-SSW trending distribution. Those decrease values towards west, so there may exist low resistivity layer at the western side. And those of less than 100 ohm-m are distributed at width of 300m at Line 270S, showing NNE-SSW trend at the western part of the block and decrease those distribution area southward. While, those of higher than 1,000 ohm-m are found at the eastern side of all survey lines, and may extend beyond the survey area.

2) n=3 (Fig. II–3–13)

At the Block North, apparent resistivities of higher than 500 ohm-m are widely distributed and those distribution area are larger than that on the n=1 map. Those of lower than 500 ohm-m are found at three locations in the northern part and at one location in the southern part independently. Those of higher than 1,000 ohm-m are found at two locations in the central part; one is distributed from Line 110S to the southeast of the block in NNW-SSE trend, and other one is distributed widely in the southern part of the block in N-S trend. These two high apparent resistivities are not found on the n=1 map, so it is suggested that high resistivity body with N-S trend may exist below the depth of –100 mGL.

At the Block South, apparent resistivities show distribution with NNE-SSW trend, and different patterns of those are found at the central part of the block. Those of higher than 1,000 ohm-m and of lower than 500 ohm-m are distributed at the eastern part and at the western part of the block, respectively.

3) n=5 (Fig. II–3–14)

Apparent resistivity distribution is similar as that on the n=3 map.

At the Block North, apparent resistivities of higher than 1,000 ohm-m, occupying half area of the block, arrange like arrowhead at the central part of the block, and increase those distribution area towards south. While, those of lower than 500 ohm-m are found independantly at the northwestern, northeastern and southern parts for the block.

At the Block South, apparent resistivities show NNE-SSW trending distributions. Those of higher than 1,000 ohm-m are found at the central to eastern parts of the block and extend to the east beyond the block, and those of lower than 500 ohm-m at the western part.

(2) P.F.E. plan map

P.F.E. values of more than 2.0% are defined to be IP anomalous values.